March 1990

THE EFFECT OF WELDING PARAMETERS ON HYDROGEN DISTRIBUTION IN PIPELINE WELDS

[PART OF THE PROGRAM OF THE FEDERAL PANEL ON ENERGY R & D (PERD)]

FINAL REPORT

Work on this project was conducted under the auspices of the Metals Technology Laboratory, Canada Centre for Mineral and Energy Technology, Energy, Mines and Resources Canada.

DSS FILE NUMBER: 009SQ.23440-9-9206

DSS CONTRACT NUMBER: 23440-9-9206/01-SQ

EMR SCIENTIFIC AUTHORITY: Dr. J.E.M.Braid

MICROMEDIA

73 pp

GRAVILLE ASSOCIATES INC.

P.O.Box 225 Georgetown Ontario L7G 4Y5 Tel: (416) 873-1739 FAX: (416) 873-0466

EXECUTIVE SUMMARY

The effect of welding parameters on the cooling time and the diffusion of hydrogen has been determined. A simple analytical method and the finite element method (FEM) were used. Both methods gave similar results but the simple method was very sensitive to the value of heat transfer coefficient.

The results showed that the relation between the hydrogen diffusion parameter (τ) and cooling time S_{100} was not unique over a wide range of conditions. In a simulated pipeline procedure τ and S_{100} were greatly affected by environment (ambient temperature and wind) but less by the welding parameters. The total width of preheating greater than 300 mm had no effect and preheat temperature had a small effect. In the presence of wind the use of blankets was shown to have a major effect.

SOMMAIRE EXECUTIF

L'effet des paramètres de soudure sur le temps de refroidissement et la diffusion de l'hydrogène a été déterminé. Nous avons utilisé une méthode analytique simple et la méthode des éléments finis (MEF). Les deux méthodes ont donné les résultats comparables mais la méthode simple a été très sensible à la valeur du coefficient du transfert du chaleur.

Les résultats ont montré que la relation entre la paramètre de la diffusion de l'hydrogène (τ) et le temps de refroidissement (S_{100}) n'était pas unique dans les grandes variations des conditions. Dans une procédure du pipe-line simulé τ et S_{100} sont affectés par l'environnement (la température ambiante et du vent) mais moins par les paramètres de soudure. La largeur totale du prechauffage plus de 300 mm a produi aucun effet et la température du prechauffage a produi un peu d'effet. En présence du vent nous avons montré que les couvertures ont produi un grand effet.

CONTENTS

Introduction	1
Background	1
Methods	2
Diffusion parameter	3
Heat flow model	4
Surface transfer coefficient	6
Single pass welds	7
Multipass welds	7
Comparison of FEM and simple model results	9
Repair weld	10
Critical concentration for cracking	11
Conclusions	12
References	13
Tables	15
Figures	17
Finite Element Method Analysis	37

THE EFFECT OF WELDING PARAMETERS ON HYDROGEN DISTRIBUTION IN PIPELINE WELDS

Introduction

There is currently considerable interest in identifying and quantifying the effects of welding procedure parameters and steel composition factors on the risk of cracking in pipeline girth welds. Of particular interest in Canada is the effect of low ambient temperatures that may be experienced during winter construction. Although low ambient temperatures are generally assumed to increase the risk of cracking there has been little work to quantify the effects and to suggest how welding procedures should be modified for winter conditions.

The present work was undertaken to calculate the effects of changes in welding parameters on the thermal cycle and the diffusion of hydrogen for a typical pipeline girth weld.

Background

It is generally believed that hydrogen cracking under a given stress level occurs when a critical concentration of hydrogen is retained in the weld or heat affected zone after it has cooled down. The main effect of procedural variables such as preheat is to modify the cooling rate such that more hydrogen diffuses from the weld before it has cooled down. This has traditionally been characterized by the cooling time from 1500°C to 100°C (S_{100}) on the assumption that this controls the amount of hydrogen remaining in the weld below 100°C. Predictions of suitable welding procedures, particularly the minimum preheat temperature, have then been made on the basis of achieving a critical cooling time S_{100}[1,2]. The effects of ambient temperature have also been analysed in terms of the cooling time S_{100} when local preheat was used[3].

Cooling time S_{100} does not, however, uniquely determine the hydrogen

content since that would imply a constant shape of the cooling curve and a constant proportion of time spent in each temperature range. Changes in welding parameters will change the shape of the cooling curve. A more generalized term τ that represents the extent of hydrogen diffusion has therefore been widely applied[4,5]. The term τ is defined as

$$\tau = \int D(T)\, dt$$

over the thermal cycle of interest. D(T) is the diffusion coefficient of hydrogen and is a function of temperature. τ is evaluated numerically and in the present work is taken down to 50°C.

For τ to be used as a cracking parameter it must be assumed that cracking depends on the average hydrogen remaining in the weld. This assumption may be reasonable for simple geometries and single pass welds but is not likely to be valid for more complex situations. There have, therefore, been many studies in the past ten years aimed at determining the distribution of hydrogen in the weld including the effects of local accumulation due to straining[6].

In the present work the effects of welding procedure variables are studied by determining their effect on cooling time S_{100} and diffusion parameter τ. The results of the thermal cycle calculations have then been applied to determine local hydrogen levels in the root of a pipeline repair weld.

Methods

Two methods of calculation have been followed. The first is an analytic approach aimed at providing approximate solutions and illustrating general trends. The second is a finite element method (FEM) used to generate more accurate solutions for specific cases. No experimental work has been undertaken in the present study. In the following part of the report the results of the analytic calculations are discussed. The FEM work is presented in a separate section.

Diffusion Parameter

To illustrate the relation between the diffusion parameter, τ and the hydrogen concentration consider (Fig. 1) the one dimensional diffusion of hydrogen in a slab ($-l<x<l$) under the boundary conditions $c = 0$ at $x = -l, l$. Assume the initial hydrogen distribution is

$$c = c_0 \cos\left(\frac{\pi x}{2l}\right)$$

The distribution after time, t is

$$c = c_0 \cos\left(\frac{\pi x}{2l}\right) \exp \frac{-D\pi^2 t}{4l^2} \qquad (1)$$

This is equivalent to considering just the fundamental term of a Fourier series. The distribution retains the cosine shape but decays exponentially.

If the temperature is changing then D changes with time. In this case the temperature/time curve can be broken into steps in each of which D can be considered constant. Equation (1) provides the solution for each step with the initial distribution being the solution for the previous step. Thus

$$c = c_0 \cos\left(\frac{\pi x}{2l}\right) \exp\left(\frac{-\pi^2 D_1 t_1}{4l^2}\right) \exp\left(\frac{-\pi^2 D_2 t_2}{4l^2}\right) \exp\left(\frac{-\pi^2 D_3 t_3}{4l^2}\right) \ldots\ldots$$

$$= c_0 \cos\left(\frac{\pi x}{2l}\right) \exp \frac{-\pi^2 \Sigma D_i t_i}{4l^2}$$

Writing $\Sigma D_i t_i = \tau$ gives

$$c = c_0 \cos\left(\frac{\pi x}{2l}\right) \exp \frac{-\pi^2 \tau}{4l^2} \qquad (2)$$

which is the same as equation (1) with Dt replaced by τ.

At the mid-thickness of the slab where x = 0 the concentration is

$$c = c_0 \exp \frac{-\pi^2 \tau}{4l^2} \qquad (3)$$

The value of c/c_0 is plotted in Fig. 2 against τ for three slab thicknesses to illustrate how the hydrogen concentration decreases with τ.

Heat Flow Model

The final weld pass is modelled using a point heat source with a correction for surface heat transfer that has been shown to provide reasonably reliable cooling rate predictions. For multipass welds the prior weld passes are modelled using plane heat sources i.e., neglecting through-thickness temperature distribution. This is believed to be a reasonable assumption since prior passes have cooled substantially before the final pass and heat transfer would be essentially two dimensional. The plane heat sources are corrected for surface transfer.

If time t is measured from the beginning of the final pass, the temperature (without surface transfer) due to a previous pass is given by

$$T_{y,t} = \frac{H}{gC\rho\sqrt{4\pi\alpha\,(t_1 + t)}} \exp\left\{-\frac{y^2}{4\alpha(t_1 + t)}\right\} \qquad (4)$$

where

H	=	heat input (J/mm)
g	=	thickness (mm)
α	=	K/Cρ is the thermal diffusivity
K	=	conductivity
C	=	specific heat
ρ	=	density
y	=	distance normal to the weld line
t_1	=	time from prior pass to final pass.

Adding the correction for the surface transfer and inserting appropriate values for the thermal properties gives

$$T_{(t)} = \frac{23.75 \times H}{g\sqrt{t_1 + t}} \exp\left(\frac{-476\,(t_1 + t)h}{g}\right) \qquad (5)$$

where h is the coefficient of surface heat transfer.

A similar approach is used to account for local preheat. Assume the preheat distribution at the beginning of welding is represented by a previous plane heat source. The preheat distribution is then described by

$$T = At_0^{-1/2} \exp\frac{-y^2}{4\alpha t_0} \qquad (6)$$

where the constant A includes the heat input to the preheat and t_0 is the time between 'depositing' the preheat source and the beginning of welding. The heat input to the preheat is not usually known so it is more convenient to express the distribution in terms of a characteristic width of preheating. The width σ is defined as the distance y from the weld line where the preheat temperature (above ambient) falls to 62% of the maximum value. Thus at $t = 0$

$$\exp\frac{-\sigma^2}{4\alpha t_0} = 0.62$$

and therefore

$$\sigma^2 = 2\alpha t_0 \qquad (7)$$

On the weld line ($y = 0$) the temperature may now be written as

$$T = T_m \frac{\sigma}{(\sigma^2 + 2\alpha t)^{1/2}} \qquad (8)$$

where T_m is the preheat temperature at t = 0 and 2α is the width of preheating.

This equation is further modified to include the effects of surface transfer to give

$$T = T_m \frac{\sigma}{(\sigma^2 + 2\alpha t)^{1/2}} \exp \frac{-2\alpha h t}{Kg} \qquad (9)$$

Note that the term 'preheat width' denoted by σ and as used in this report represents half the width actually heated.

Surface Transfer Coefficient

In the above equations h is a constant and it is assumed that heat loss is proportional to the temperature difference between the surface and ambient (Newton's Cooling Law). Measured values of h, however, vary widely since the mechanisms of heat loss can change with temperature.

For calculating cooling rates at higher temperatures (e.g., $S_{800\text{-}500}$) for open arc processes, values of h ~ 80 watts/m^2/s°C appear to work quite well. For submerged arc which looses less heat by radiation because of the flux blanket, a value of h ~ 25 watts/m^2/s°C is appropriate. For lower temperature cooling rates a lower value would be expected. For cooling of preheated plates Satoh[1] used a value h = 1.08 watts/m^2/s°C. Graville[7] measured the value of h over a range of temperatures for preheated plates cooling in normal still air conditions. The value at 100°C was 11.3 watts/m^2/s°C.

When wind is present the value is expected to increase, and a detailed examination of the effect is reported in the section on the FEM analysis. For the analytical approach here the value of h was estimated to increase to about 15 watts/m^2/s°C for a wind speed of 25 kph. The value of k was also included as one of the variables in the sensitivity calculations.

Single Pass Welds

Calculations for single pass welds were done primarily to determine whether cooling time to 100°C (S_{100}) was uniquely related to τ over a wide range of welding conditions. The variables included in the calculations were energy input, thickness, preheat, and ambient temperature. The width of preheat was constant at 150 mm and h was taken as 10 watts/m^2/s°C for the preheat.

Results are given in Table 1 and cooling time to 100°C is shown plotted against τ for all results in Fig. 3. For small values of S and τ there is a good correlation but there is wide divergence at higher values. The points at higher values appear to diverge roughly on the basis of thickness. This might be expected since a thinner plate spends proportionately more time at lower temperatures (below the transformation) and would provide a bigger contribution to hydrogen diffusion (τ) for a given cooling time. The scatter, however, is sufficiently large that cooling time to 100°C cannot be considered as given an accurate measure of hydrogen diffusion.

Multipass Welds

A typical pipeline girth weld was used as a model for the multipass weld calculations. The procedure is given in Table 2. The variables that were explored were preheat temperature, preheat width, ambient temperature, and heat transfer coefficient. The latter would provide information on the effect of wind or insulating blankets. In all calculations the time (and τ) is measured from the deposition of the capping pass.

In Fig. 4 the effect of surface transfer coefficient on cooling time is given and the effect on τ is presented in Fig. 5. In the latter graph the kink in the curves is the result of a residual error in the estimation procedure in the program. The data is given for ambient temperatures of 20°C and –20°C with a preheat of 150°C and a preheat width of 150 mm. The results show a dramatic effect of surface coefficient

suggesting that factors such as wind would markedly affect the diffusion of hydrogen. Similarly cutting the transfer coefficient by 50% by insulation could more than double τ and the cooling time under some conditions.

In Figs. 6 and 7 the effect of preheat temperature is shown for a preheat width of 150 mm. Results are presented for 20°C ambient with no wind (h = 10 $W/m^2/s°C$) and –20°C with wind (h = 15 $W/m^2/s°C$). These two cases were selected as representing favourable (summer) conditions and unfavourable (winter) conditions.

The results show a relatively small effect of preheat temperature, particularly under wind conditions. This is because in the procedure used much of the preheat has been lost by surface transfer before the final pass is made. Each pass is made before the temperature drops below 150°C so the interpass of 150°C is maintained. But this is maintained largely by the heat of the welds and not the original preheat. As the value of h drops (for example, by using insulation) so the effect of preheat increases. It is of interest to note that in the graphs shown an increase in preheat temperature in the range 100°C to 200°C cannot counteract the effects of an adverse environment.

In Figs. 8 and 9 the effect of changes in preheat width σ (i.e., half the actual width heated) are shown. The effect levels off as the width increases and widths greater than about 200 mm appear to offer little extra benefit. Again, the effect is greatest for conditions of low surface transfer where most heat loss is by conduction in the pipe. The results also show again that the effect of adverse conditions (–20°C with wind compared with 20°C without wind) cannot be offset by simply increasing the preheat width.

The effect of ambient temperature at two values of h (h = 10 $W/m^2/s°C$) for no wind and 15 $W/m^2/s°C$ for wind) is shown in Figs. 10 and 11. There is a substantial decrease in the cooling time as the ambient temperature drops, although the effect on τ is less marked. The effect of surface transfer coefficient, however,

still dominates and the cooling time or τ at 20°C with wind is about the same as that at –30°C without wind.

All results from the multipass runs are plotted in Fig. 12 as cooling time S_{100} against against τ. A reasonable correlation is evident and far better than for the single pass runs. This might be expected since all the multipass runs were on the same thickness. Fig. 13 shows results from both sets of calculations plotted together. For the limited range of variables used on a single thickness pipe the cooling time to 100°C would be a useful guide for estimating τ and the effect on hydrogen diffusion.

Comparison of FEM and Simple Model Results

The results of the FEM calculations are presented in a separate section. Although the two models differ slightly in their initial assumptions a comparison between the two is of interest. The FEM model used a four pass welding procedure in which the final pass was effectively a combination of the two last passes of the simple model discussed here. The FEM model also assumed a uniform preheat temperature over the preheat width whereas the simple model used a distribution. In the FEM model the term "preheat width" is the total heated width whereas in the simple model it is the characteristic half width. These differences make it unlikely that results of the two methods would agree exactly.

Cooling times in the simple model were calculated from deposition of the final weld but two cooling times are reported for the FEM model: that of the root pass calculated from when the root pass reached 1500 °C and that for the final pass when it reached 1500 °C. If the time between passes of 1200 seconds is subtracted from the root pass cooling times there is rough agreement between the two values from the FEM model with the root pass cooling time being about 50 to 100 °C longer than that of the final pass. When compared with figures from the simple model the latter are generally 20 to 50% higher. This also applies to the corresponding τ values. Part of this discrepancy may rest with the preheat width used. In fact, the

values of τ are within 4% for the two models when the same width of preheat is used despite the difference in temperature profile. There was, however, only one result for this case. The discrepancy between the models also seems to be higher when wind is considered. This is probably because of the values of the heat transfer coefficient assumed in the simple model. Comparison of the FEM results with those of the simple model shown in Figure 4 (effect of heat transfer coefficient) would allow appropriate values of h to be selected to "calibrate" the simple model.

Overall the agreement between the two approaches is considered quite good and in any event they predict the same trends and similar sensitivities to changes in welding procedural parameters.

Repair Weld

In order to determine the effects of procedure variables on the local hydrogen concentration, the thermal cycle calculations were used as an input to a simple finite difference model (FDM) for hydrogen distribution. The FDM approach assumes one dimensional diffusion of hydrogen through the weld where the concentration is taken as zero at the free surfaces. The model accounts for the hydrogen introduced by each weld bead as it is deposited. Fig. 14 illustrates the diffusion model.

The model assumes constant through thickness temperature which is a reasonable assumption for the later stages of diffusion. To avoid exaggeration of the extent of diffusion at the root when the final passes are deposited the temperatures of each pass are 'capped' at some estimated peak temperature.

Two conditions were run: 20°C ambient with no wind and –20°C ambient with wind. Hydrogen concentrations in the root region which is a likely crack initiation location, were determined. Fig. 15 and Fig. 16 show the thermal cycles for each case where time is now measured from the beginning of welding the first pass. The cycles differ, as expected, mainly in the rate of cooling to ambient after the final pass.

Hydrogen concentration (relative to the initial value) is plotted in Figs. 17 and

18. as the repair welding progresses there is a buildup in the root region, both cases following the same pattern during the buildup and reaching the same peak value. Following the final pass, however, the 20°C ambient case shows a marked drop in hydrogen as it cools to ambient. In contrast, the hydrogen level in the –20°C case remains at a relatively high level as the weld cools. There is, therefore, a clear tendency to retain more hydrogen when the ambient is lower and the cooling rate faster.

Of more significance is the amount of hydrogen retained as the weld cools to specific temperatures regardless of the time after welding. The results have therefore been plotted in the form of hydrogen concentration versus the reciprocal of the absolute temperature in Figs. 19 and 20.

Critical Concentration For Cracking

Most models of hydrogen cracking in welds assume that cracking occurs when a critical hydrogen content is exceeded below a specific temperature, e.g., 50°C or 100°C. The critical hydrogen content is dependent on the stress and the composition (and microstructure) of the heat affected zone. However, it is well known that hydrogen embrittlement is very sensitive to temperature with the critical hydrogen content required for cracking under a given stress increasing with temperature. Thus, critical conditions are not always reached at the same temperature. To establish whether critical conditions are met (at constant stress) it is necessary to find the intersection of the weld hydrogen/temperature curve with the critical hydrogen/temperature curve. Unfortunately, there is little published information on the effects of temperature, and the critical hydrogen levels are generally not known. The concept can, however, be illustrated by establishing critical hydrogen curves for arbitrary stresses based on the early published work on the effects of temperature[8].

It was found that the critical hydrogen concentration could be expressed as:

$$\log C_c = \frac{-1848}{T} + \text{const.}$$

or

$$C_c = A \exp \frac{-1848}{T} \qquad (10)$$

where the constant A would include the effect of stress.

This applies to one particular steel, but it can be argued that if the term exp–1848/T represents some thermal activation process exp –Q/kT, then the value of Q should be independent of steel type if the mechanism of the thermal effect is the same. This equation should apply to any steel with the relative sensitivity of the steel to embrittlement being contained in the constant A.

On this basis critical hydrogen curves for arbitrary stresses have been drawn on Figs. 19 and 20. It is now possible to explain the effects of ambient temperature in terms of the intersection of the curves. In the case of 20°C ambient, critical conditions would be met for stresses 1 and 2 but not for stress 3. For –20°C ambient with the same critical hydrogen curves, it is seen that critical conditions are met for all three stresses.

It should be noted that the critical hydrogen curves are quite steep and for –20°C ambient critical conditions would still have been met for stress 3 even if the hydrogen concentration curve was lower. This view is a departure from the conventional interpretation where it is assumed that the principal effect of a low ambient temperature is increasing the cooling rate and retaining more hydrogen below 100°C. The present view suggests that the effect of ambient temperature on the critical hydrogen concentration must also be considered.

Conclusions

Calculations have been made using an existing simple analytic model for heat flow in a weld to explore the effects of welding parameters on the cooling time and the diffusion of hydrogen. Hydrogen diffusion has been characterized by the parameter τ. The results show that surface heat transfer has the greatest effect and small changes in the value of h (the heat transfer coefficient) due to wind or the use of insulating blankets have a greater effect than small changes in preheat

temperature or width of preheating. The results suggest that adverse environmental conditions (e.g., winter welding with low ambient temperature and wind) cannot be counteracted by modest increases in preheat temperature or width of preheating.

Local hydrogen concentration in the root region of a pipeline repair weld has been determined using a simple finite difference model for two environmental conditions: 20 °C ambient with no wind and –20 °C ambient with wind. It is concluded that substantially more hydrogen is retained at lower temperatures in the latter case than in the former. However, it is also concluded that retained hydrogen alone is an insufficient criterion for cracking since the critical hydrogen content under a given stress may increase rapidly with temperature. Ambient temperature may therefore have a direct effect on cracking by its effect on the critical hydrogen level independent of any effect on cooling time or retained hydrogen content.

References

1) Satoh, K., Matsui, S., Ito, Y., Bessyo, K., Sakurai, R., and Takahara, S. "Determination of Preheating Conditions to Avoid Weld Cracking in Steel Construction," IIW-IX-730-71.

2) Yurioka, N., Suzuki, H., Ohshita, S., and Saito, S. "Determination of Necessary Preheating Temperature in Steel Welding," *Welding Journal,* Vol. 62, No 6. Research Supplement, June 1983, pp. 147-s to 153-s.

3) Suzuki, H., and Yurioka, N. "Weldability of Line-pipe Steels and Prevention of Cracking in Field Welding," IIW-IX-1458-87.

4) McParlan, M. and Graville, B.A., "Hydrogen Cracking in Weld Metals," Welding Journal, vol 55, No 4 (April 1976) Res. Sup. pp 95-s to 102-s.

5) AWS D1.1 - 86, "Guideline on Alternative Methods for Determining Preheat."

6) Yurioka, N., "A Review of Numerical Analysis on the Hydrogen Diffusion in

Welding of Steel," IIW-Doc.IX-1553-89.

7) Graville, B.A., "Cold Cracking Control," Pub. Dominion Bridge Company Ltd. Montreal 1975.

8) Graville, B.A. "Effect of Hydrogen Concentration on Hydrogen Embrittlement," *British Welding Journal*, Vol. 15, No. 4. April 1968, pp. 191-195.

Table 1. Results of calculations for single pass welds

Ambient	Preheat	Thickness	Energy input	S_{100}	τ
°C	°C	mm	J/mm	s	mm^2
20	20	10	500	81.3	0.20
			1000	175	0.55
			3000	405	1.05
		20	500	32.5	0.108
			1000	93.5	0.25
			3000	366	1.14
		40	500	30.5	0.095
			1000	66.4	0.19
			3000	203	0.68
	150	10	500	708	1.61
			1000	761	2.02
			3000	891	2.97
		20	500	1042	2.00
			1000	1110	2.23
			3000	1299	3.58
		40	500	1408	2.67
			1000	1485	2.81
			3000	1729	3.86
–20	20	10	500	78.2	0.193
			1000	164	0.525
			3000	377	0.965
		20	500	32.1	0.103
			1000	91.0	0.238
			3000	338	1.07
		40	500	30.2	0.095
			1000	65.2	0.187
			3000	193	0.64
	150	10	500	538	1.25
			1000	597	1.65
			3000	737	2.54
		20	500	756	1.41
			1000	829	1.62
			3000	1024	2.91
		40	500	975	1.73
			1000	1050	1.86
			3000	1285	2.84

Table 2. Procedure used for the multipass welds

Thickness 10 mm

Pass	Energy input	Welding time	Time before last pass
1	1,200 J/mm	5 mins	1140 s
2	1,100 J/mm	4 mins	840 s
3	1,500 J/mm	5 mins	600 s
4	1,500 J/mm	5 mins	300 s
5	2,000 J/mm	7 mins	

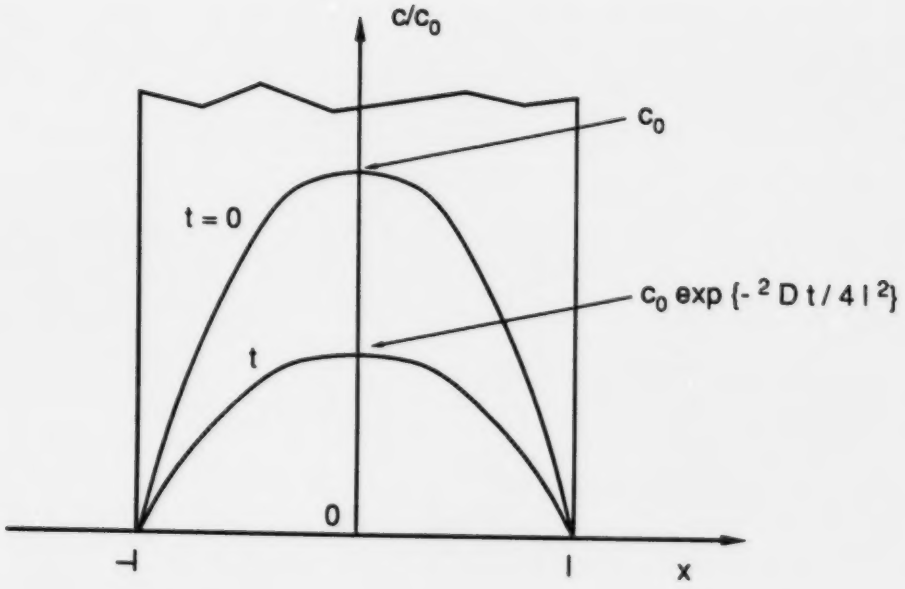

Figure 1. One dimensional diffusion of hydrogen from a slab.

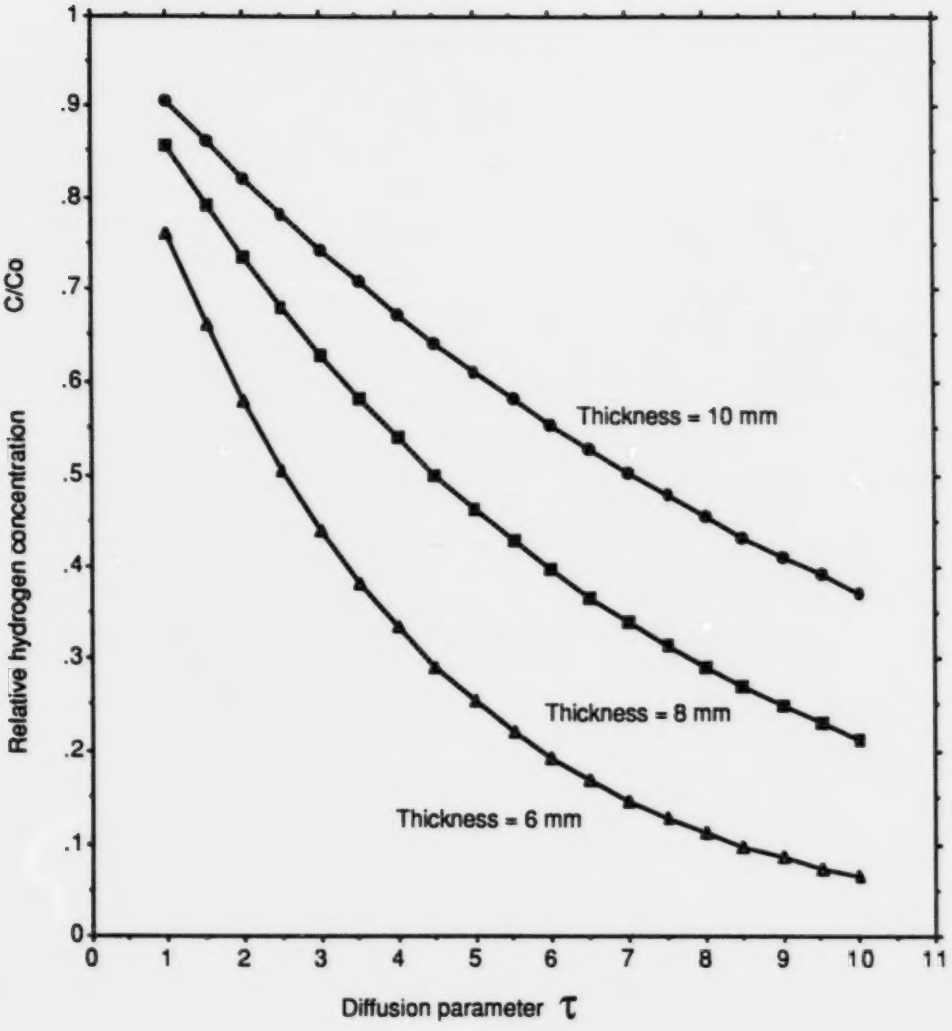

Figure 2. Hydrogen concentration at the centre of the slab as a function of τ (mm^2).

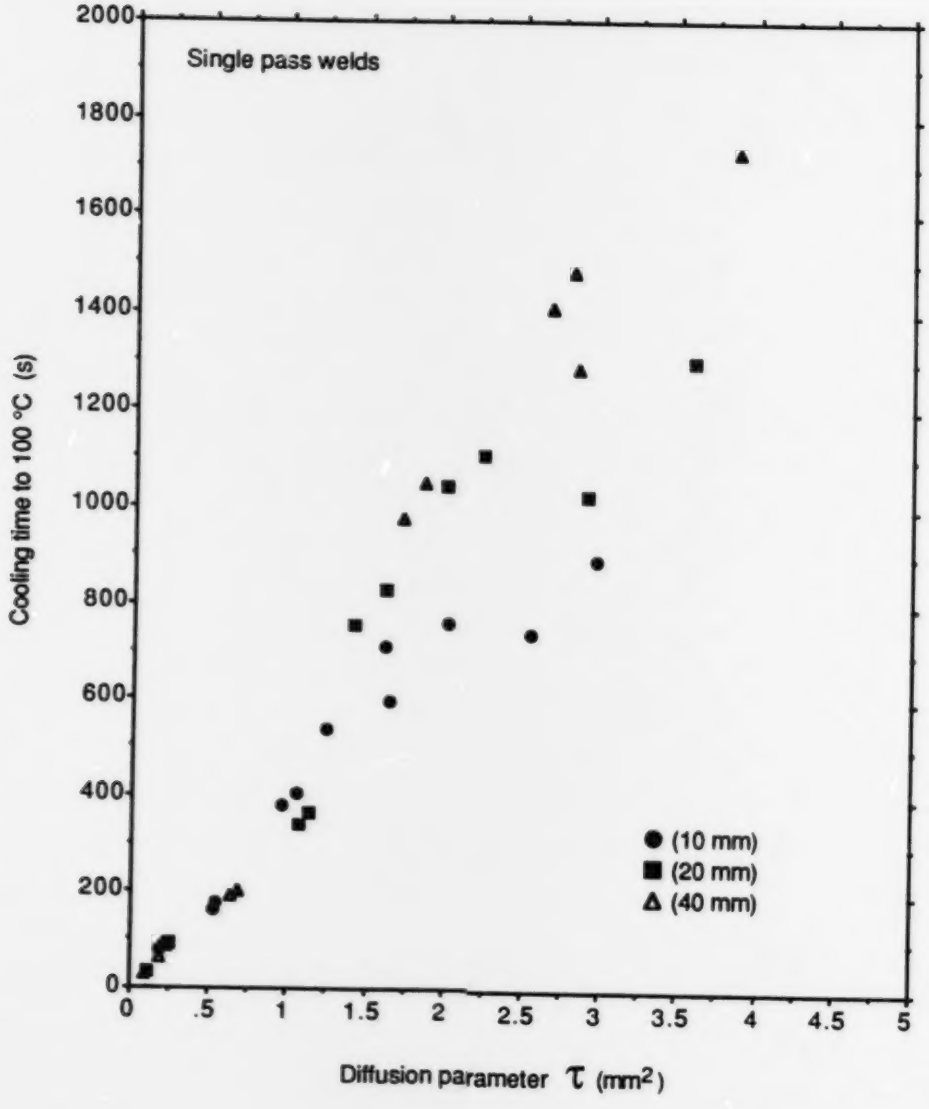

Figure 3. Relation between cooling time to 100 °C and τ for single pass welds.

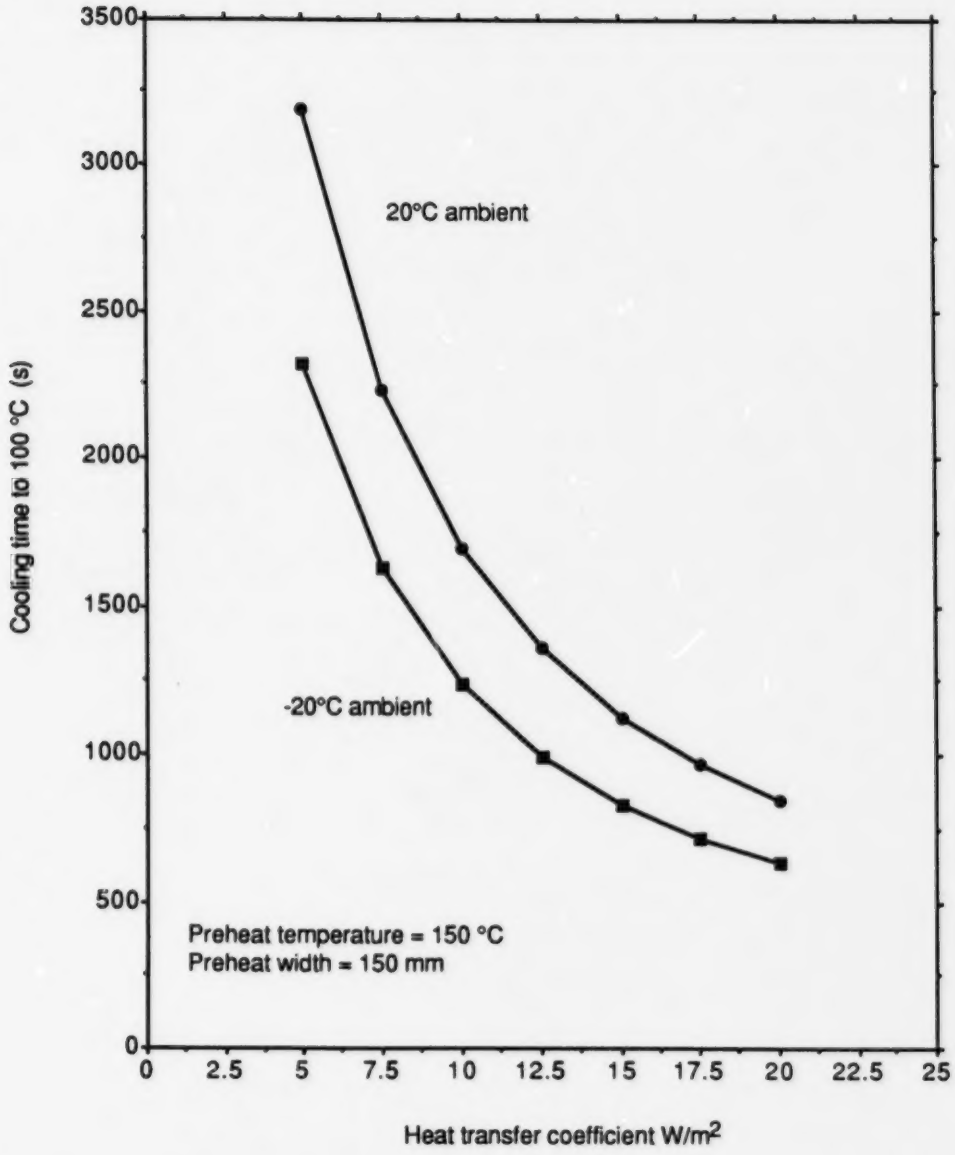

Figure 4. Effect of heat transfer coefficient on cooling time (multipass weld)

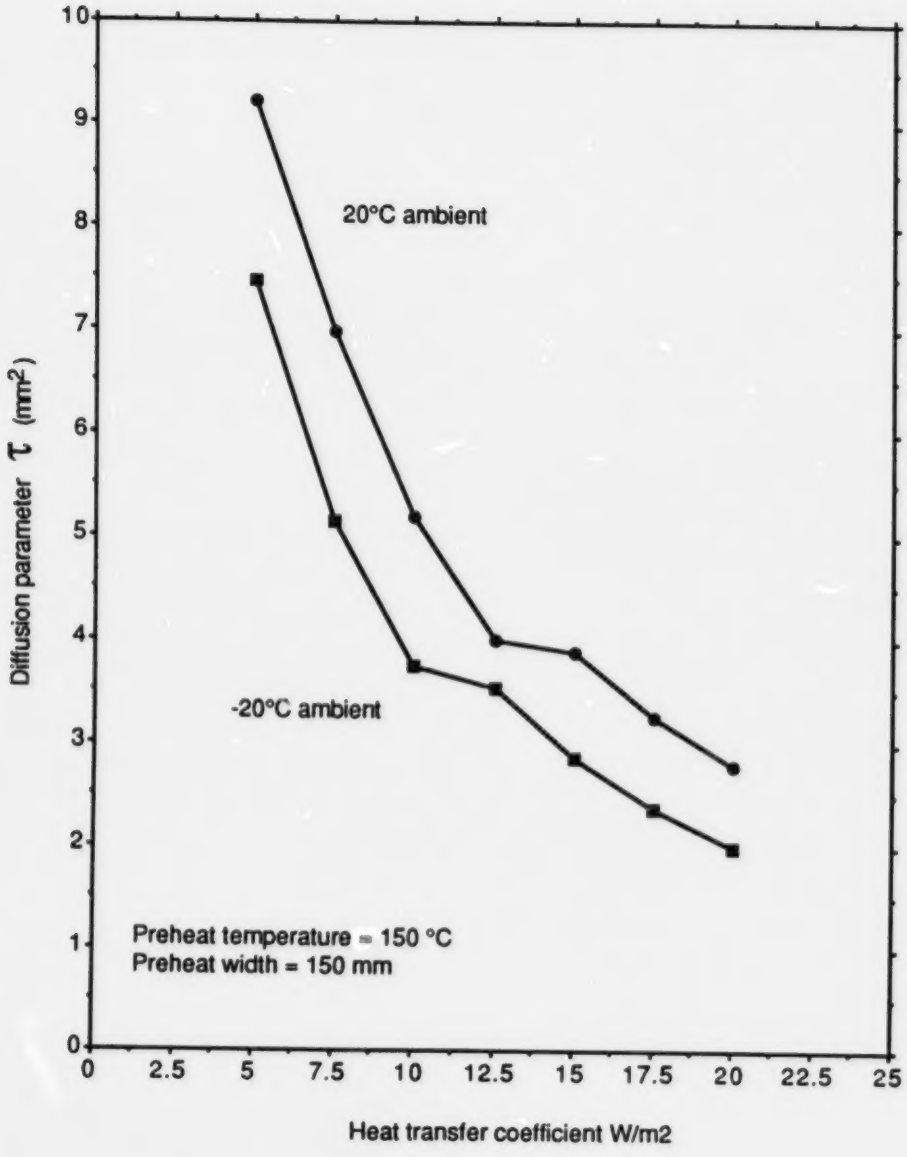

Figure 5. Effect of heat transfer coefficient on τ (multipass weld).

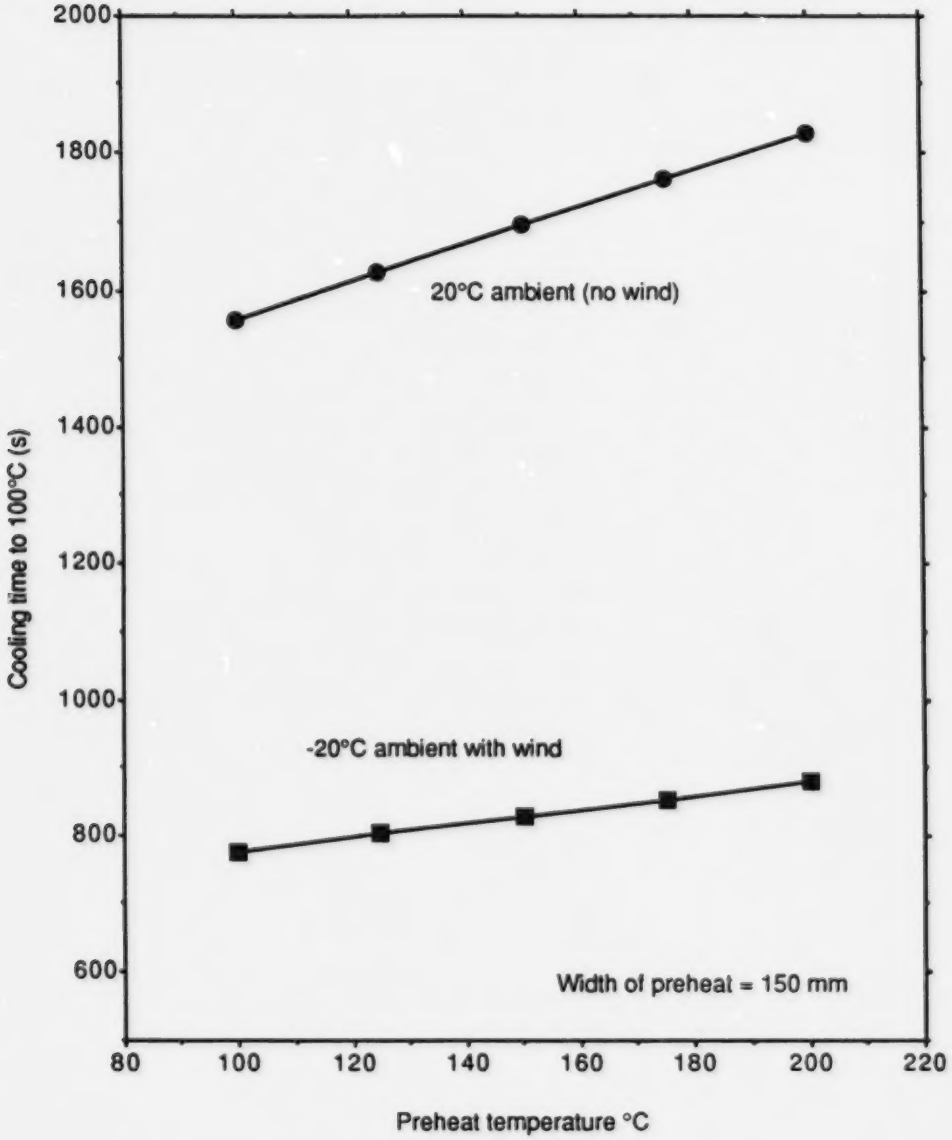

Figure 6. Effect of preheat temperature on cooling time to 100 °C.

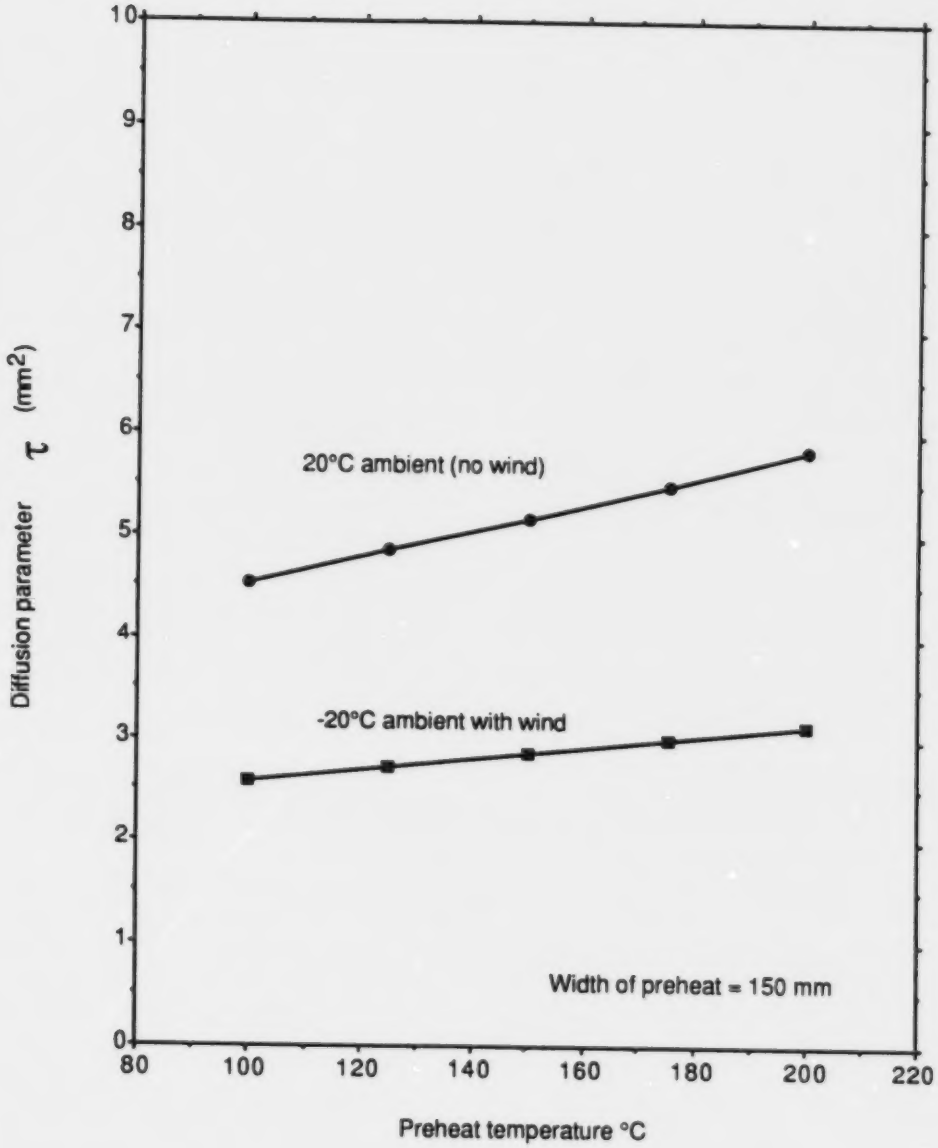

Figure 7. Effect of preheat temperature on τ.

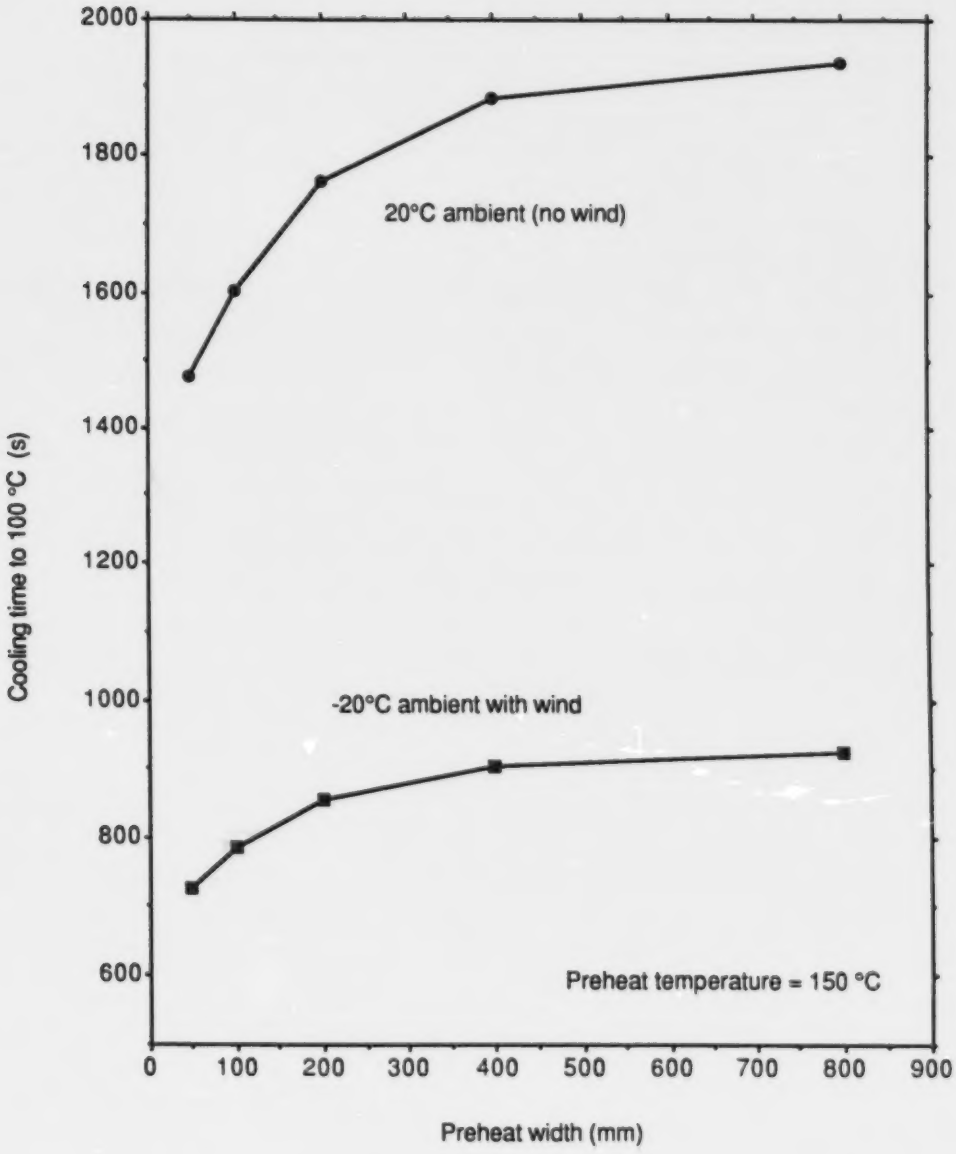

Figure 8. Effect of preheat width σ (half heated region) on cooling time.

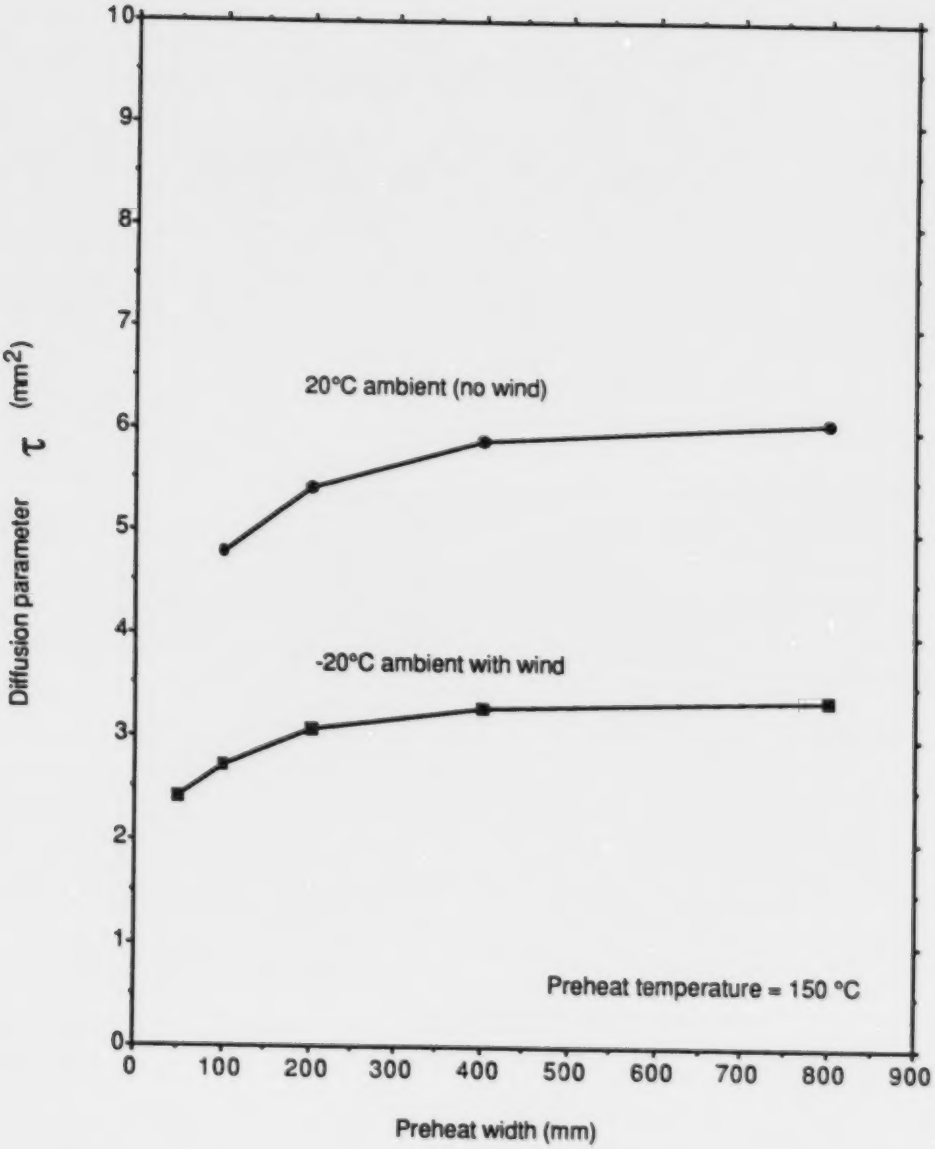

Figure 9. Effect of preheat width σ (half heated region) on τ.

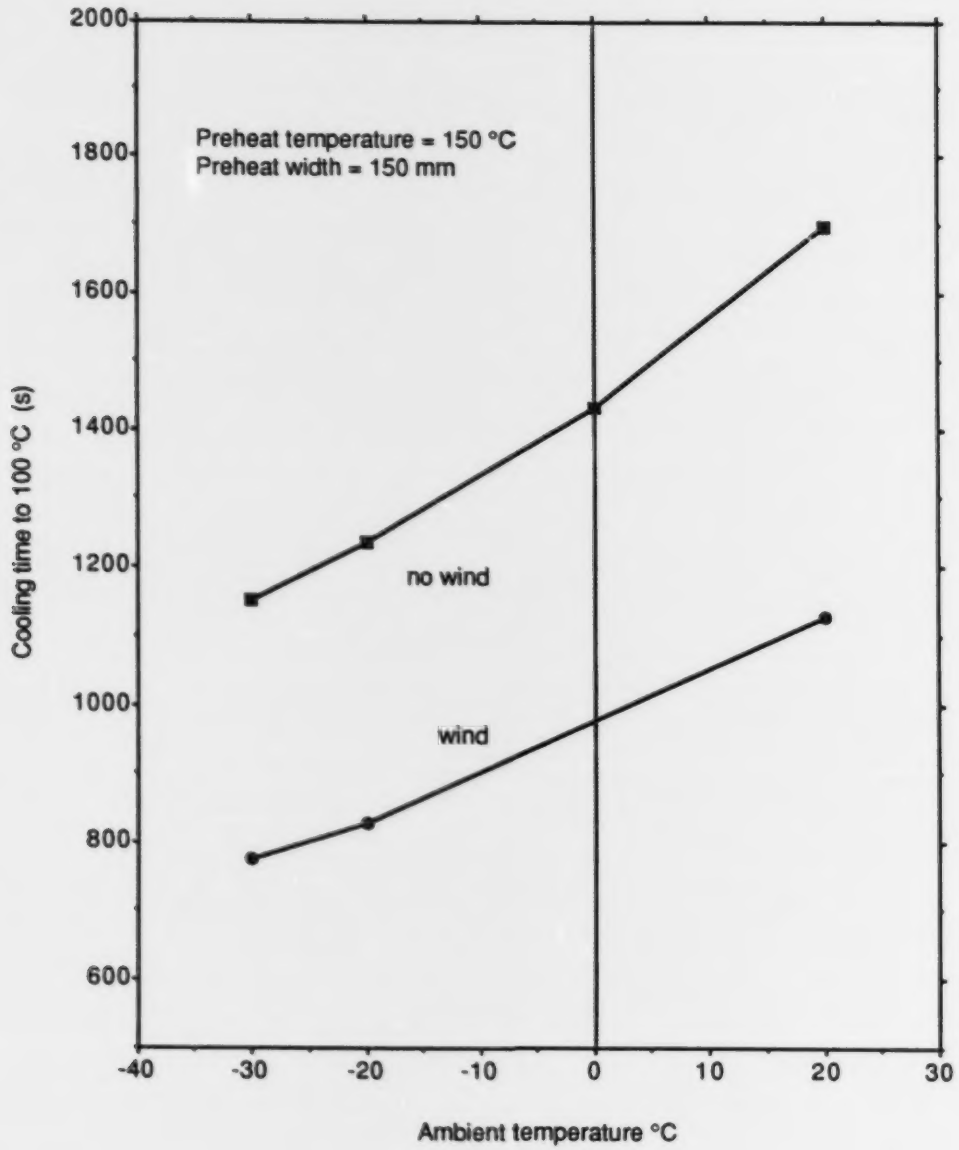

Figure 10. Effect of ambient temperature on cooling time for two values of heat transfer coefficient (h = 10, no wind and h = 15, wind).

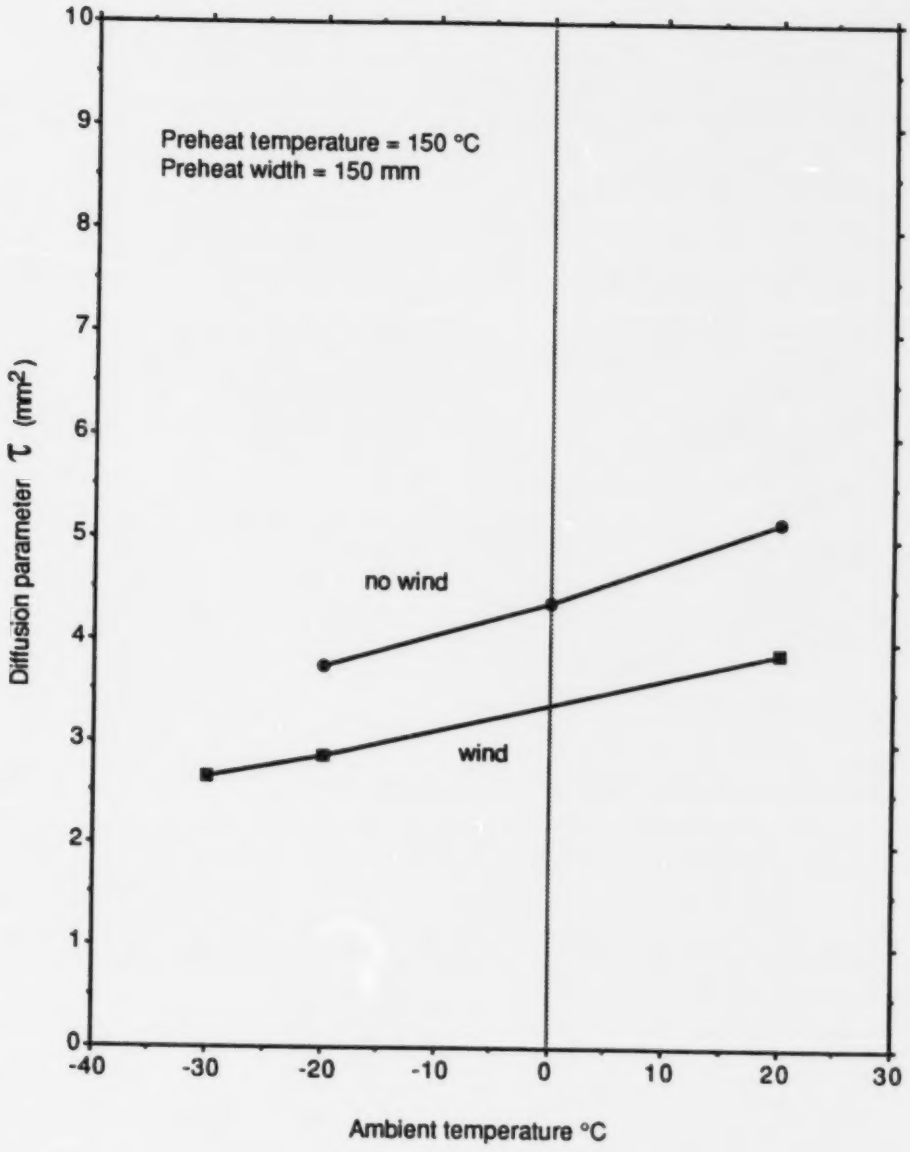

Figure 11. Effect of ambient temperature on τ for two values of heat transfer coefficient (h = 10, no wind and h = 15, wind).

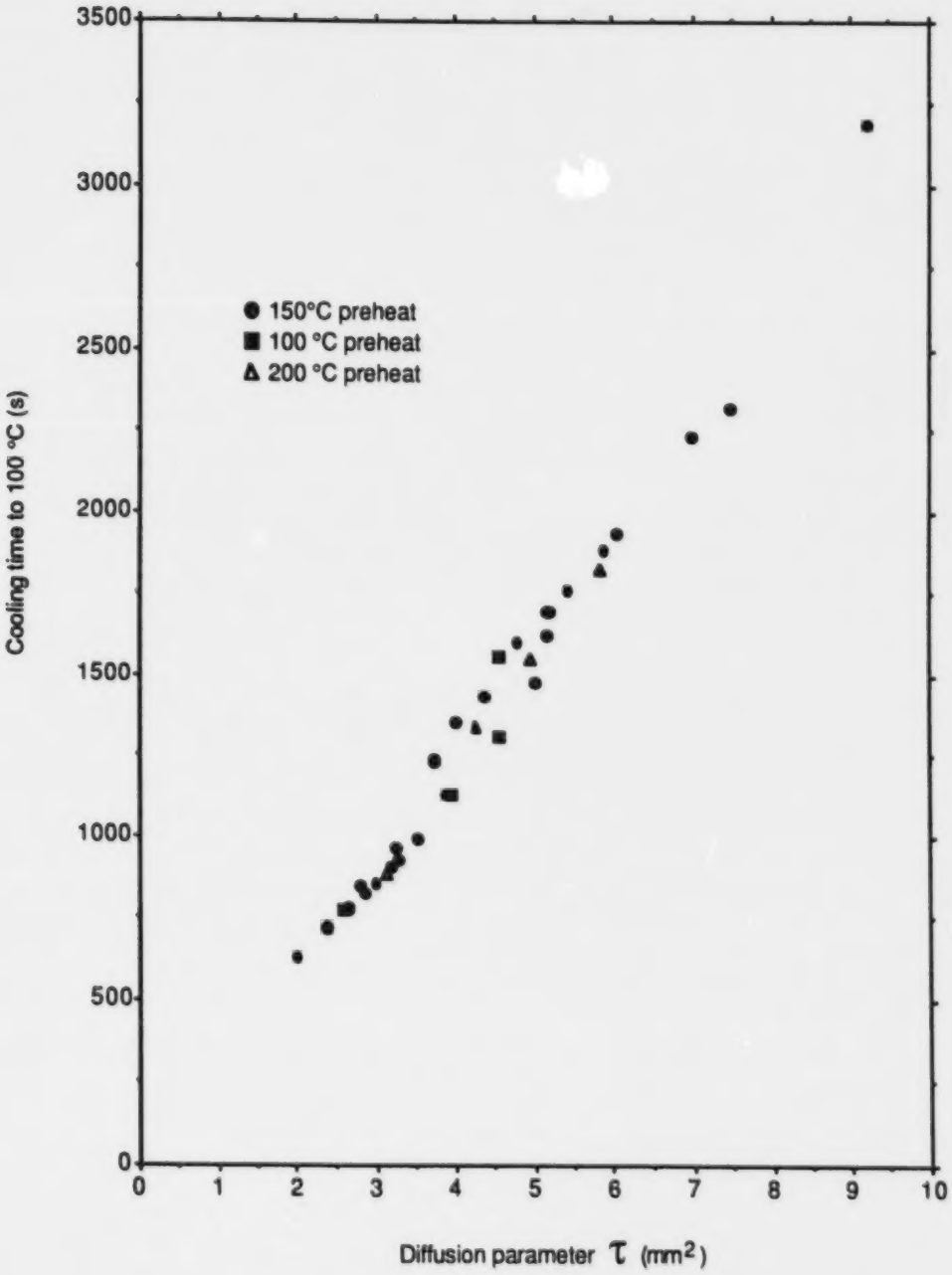

Figure 12. Relation between cooling time to 100 °C and τ for multipass welds in 10 mm pipe.

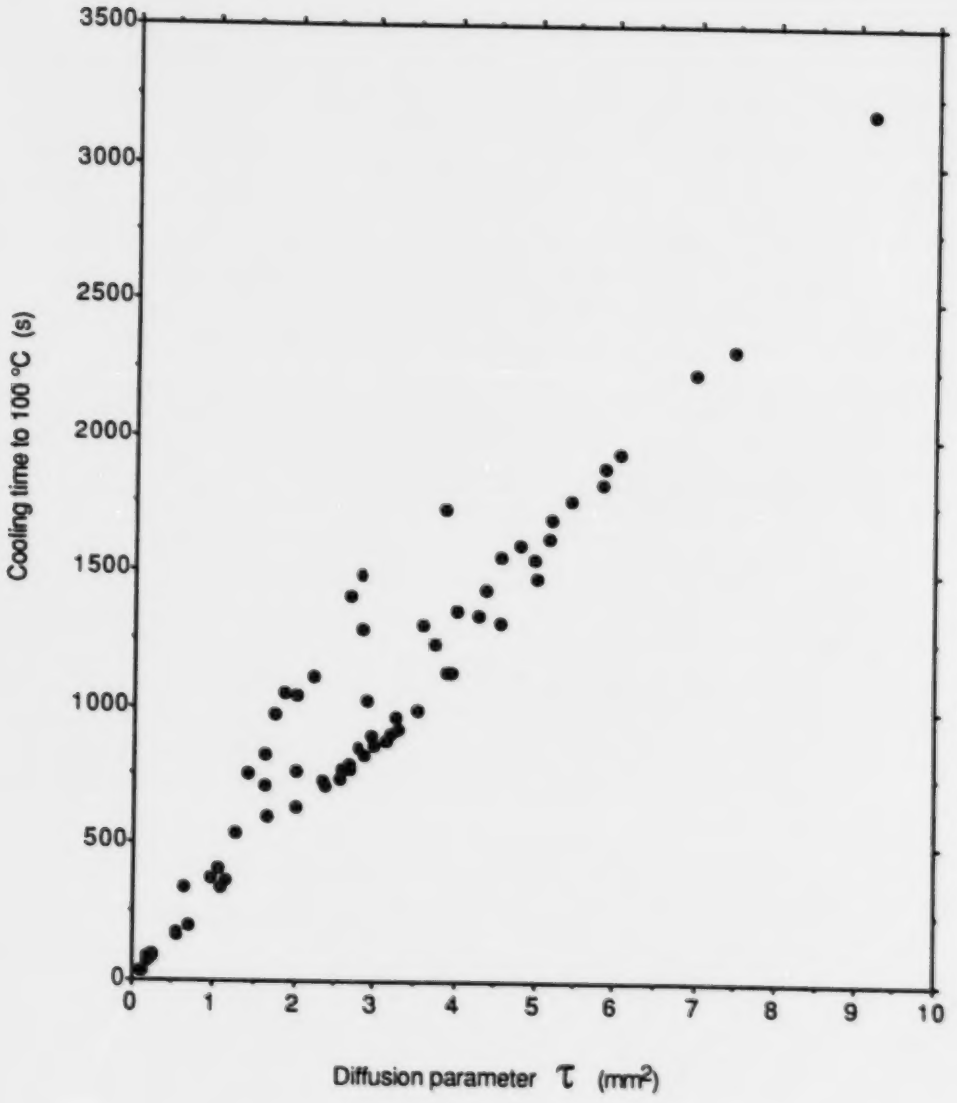

Figure 13. Relation between cooling time to 100 °C and τ for all results (single and multipass welds).

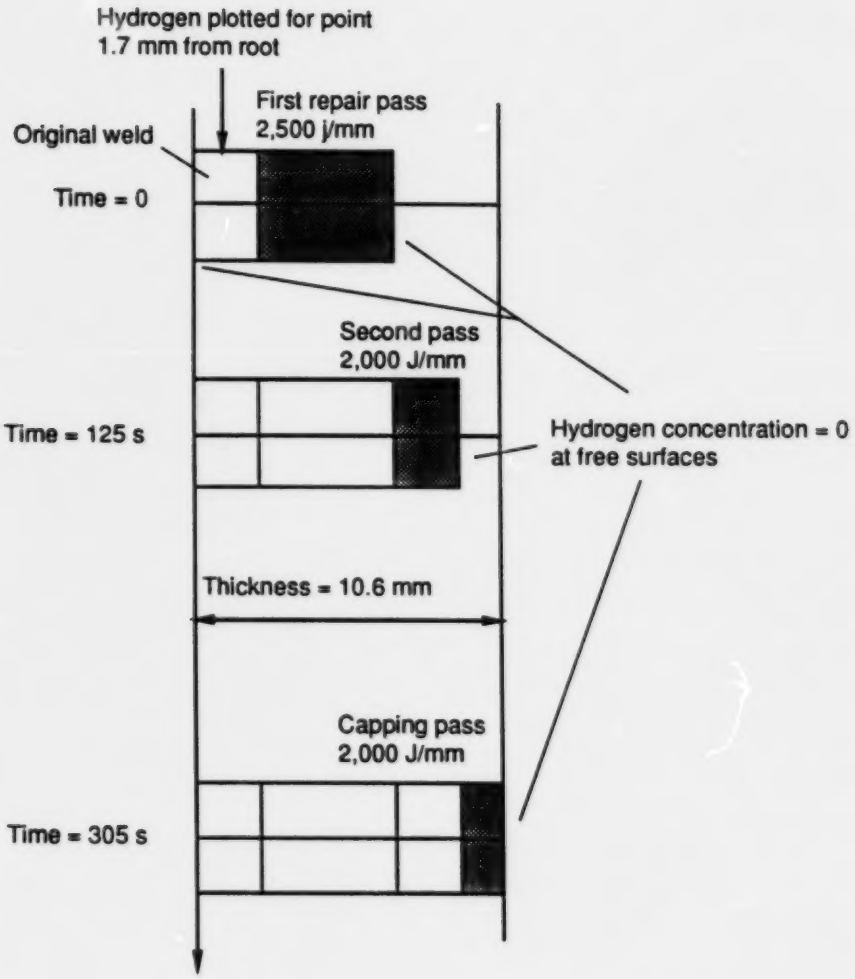

Figure 14. Model of repair weld used for finite difference analysis.

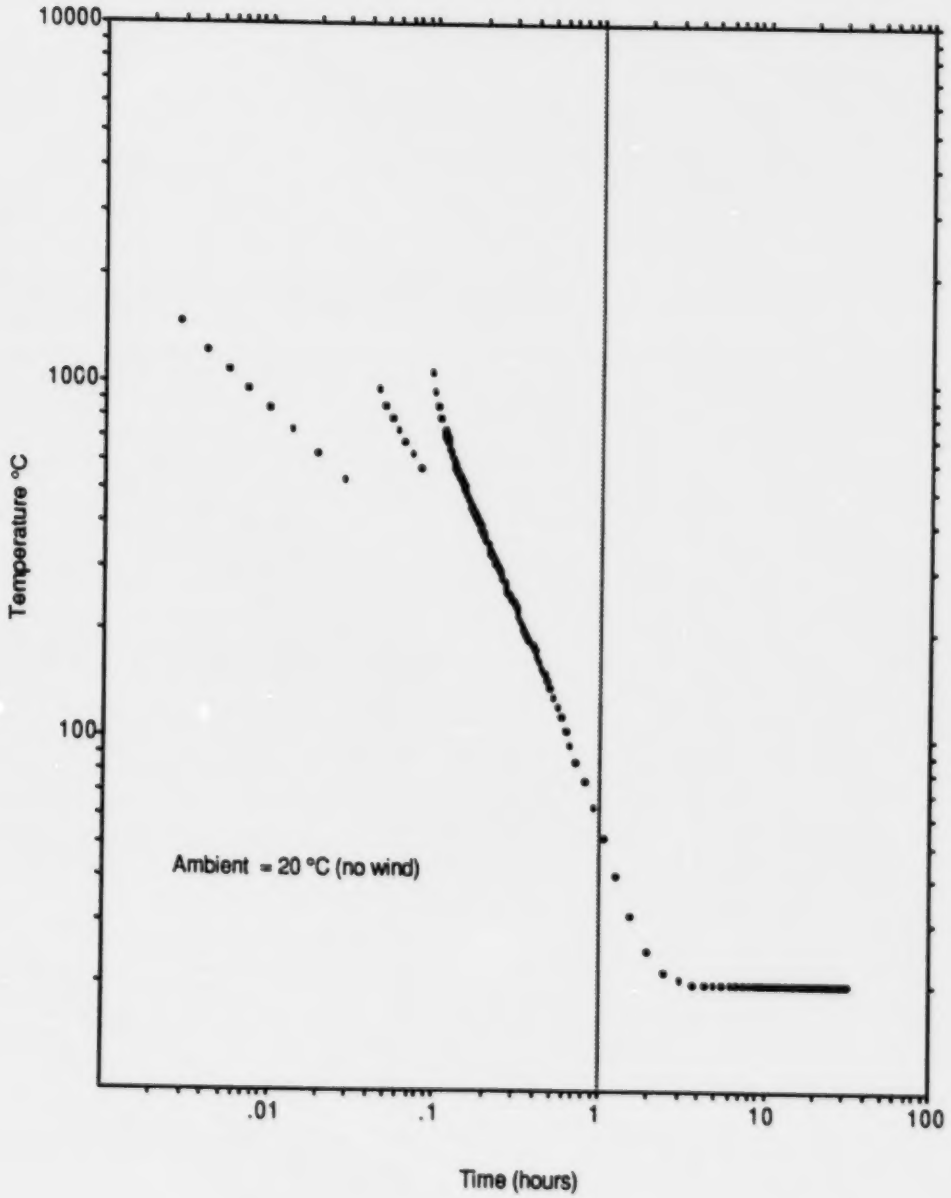

Figure 15. Thermal cycle for repair weld at 20 °C ambient (no wind).

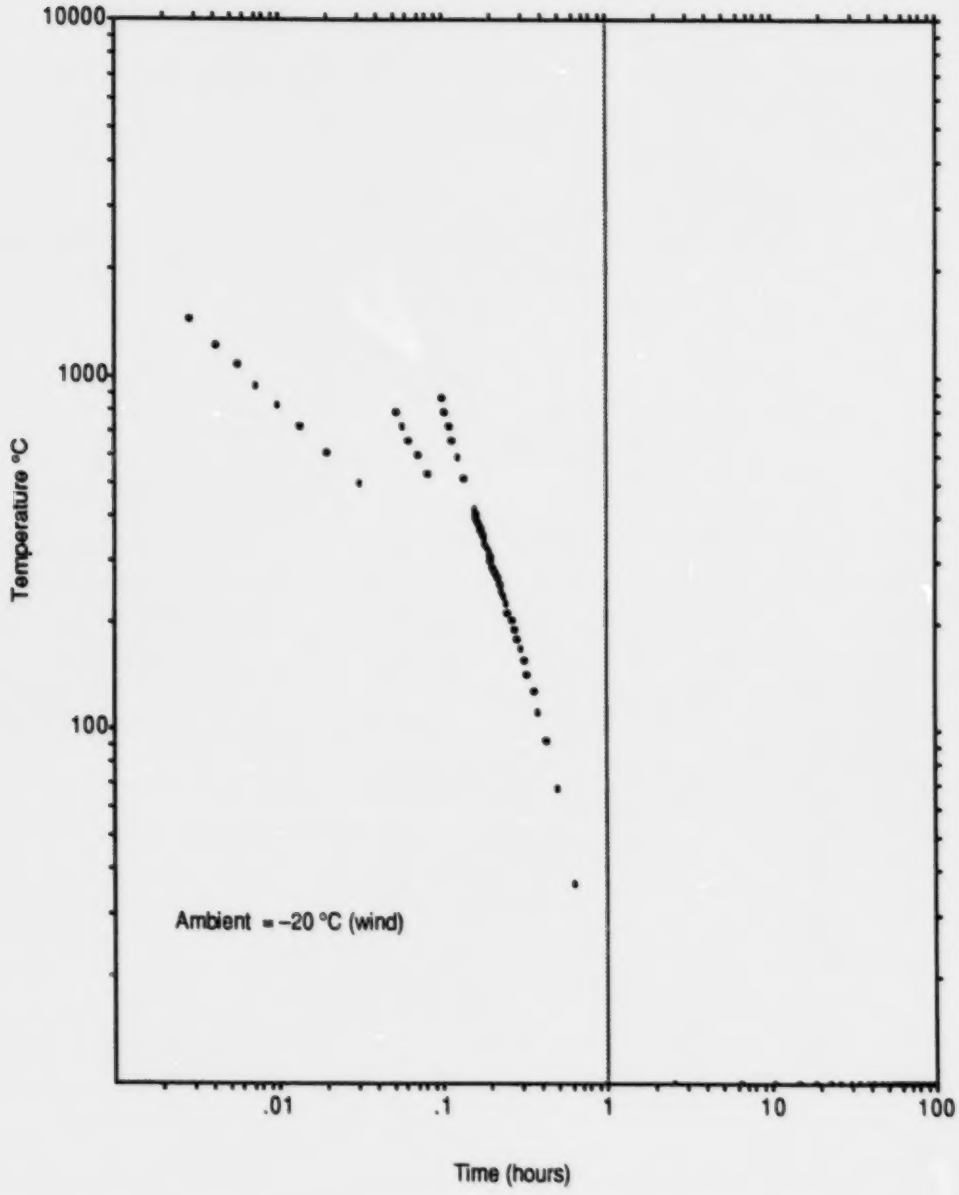

Figure 16. Thermal cycle for repair weld at –20 °C ambient (with wind).

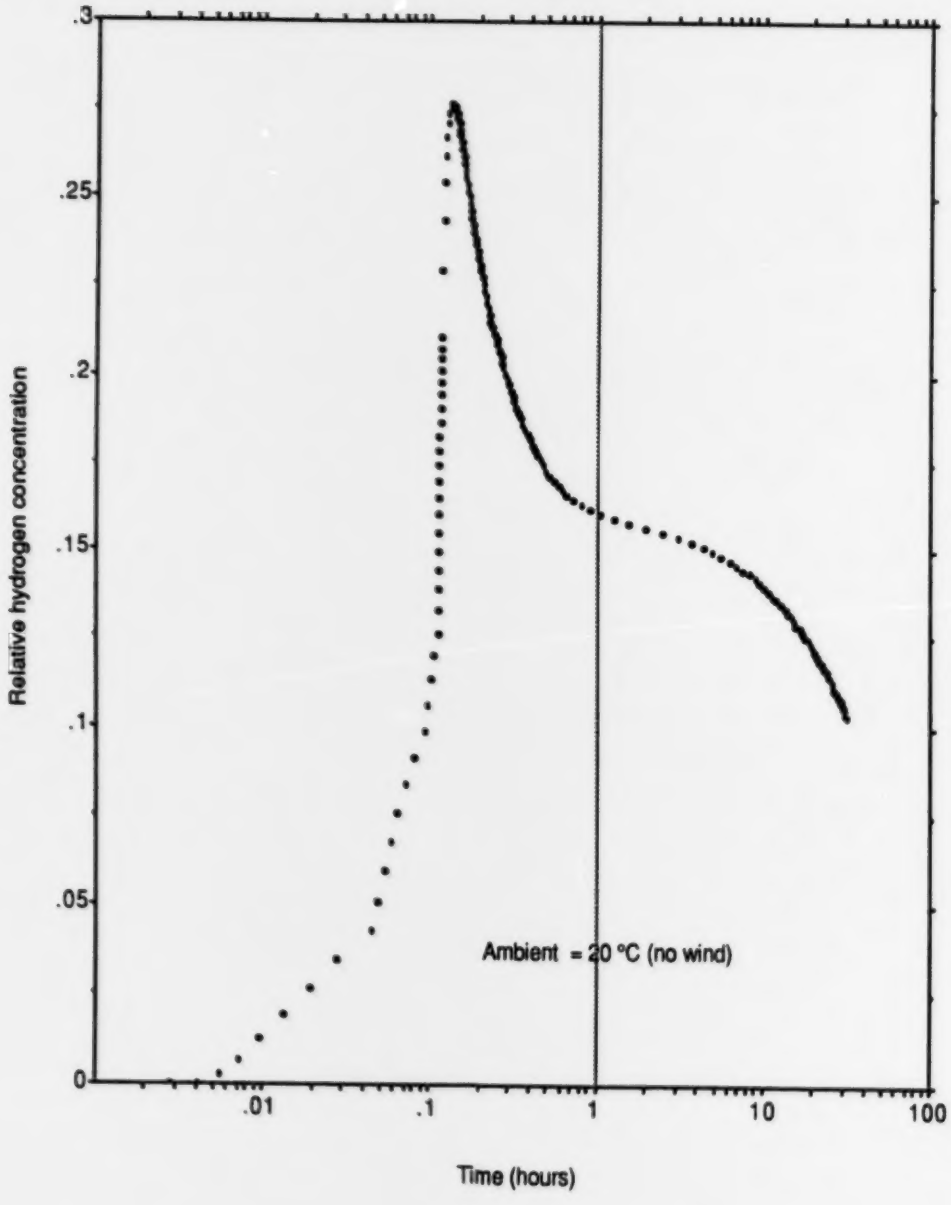

Figure 17. Relative hydrogen concentration for repair weld at 20 °C ambient.

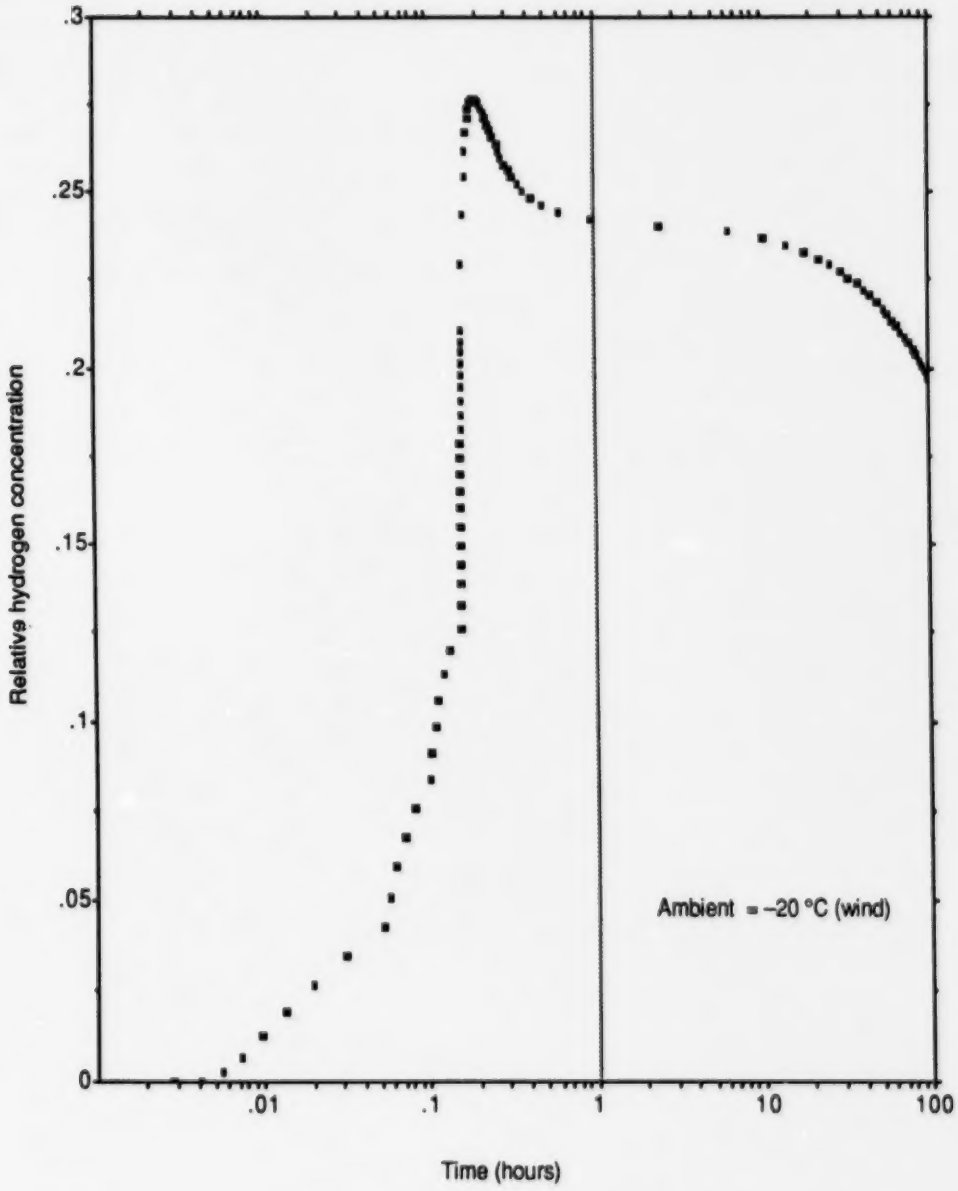

Figure 18. Relative hydrogen concentration for repair weld at –20 °C ambient.

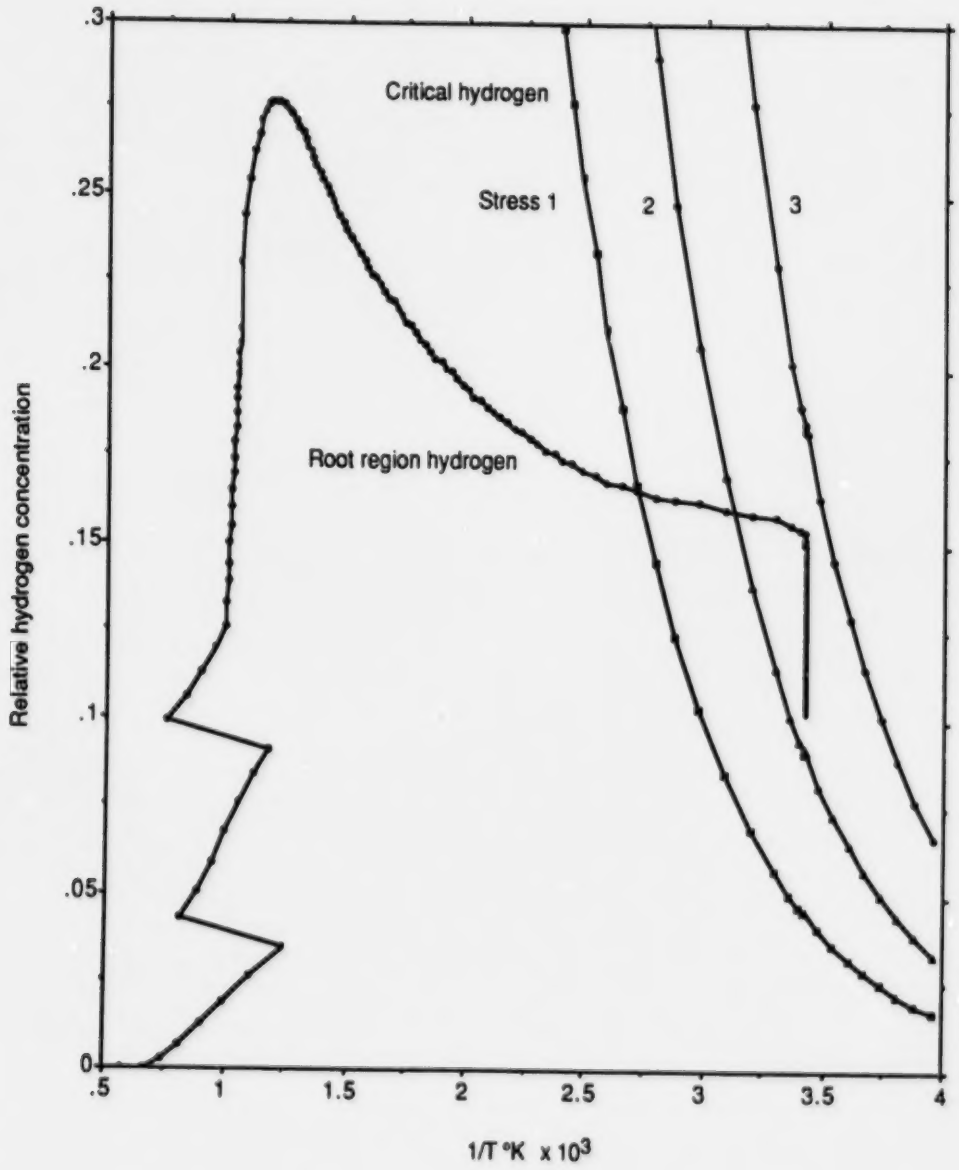

Figure 19. Relative hydrogen concentration against the reciprocal of the absolute temperature for the repair weld at 20 °C with illustration of the critical hydrogen curves.

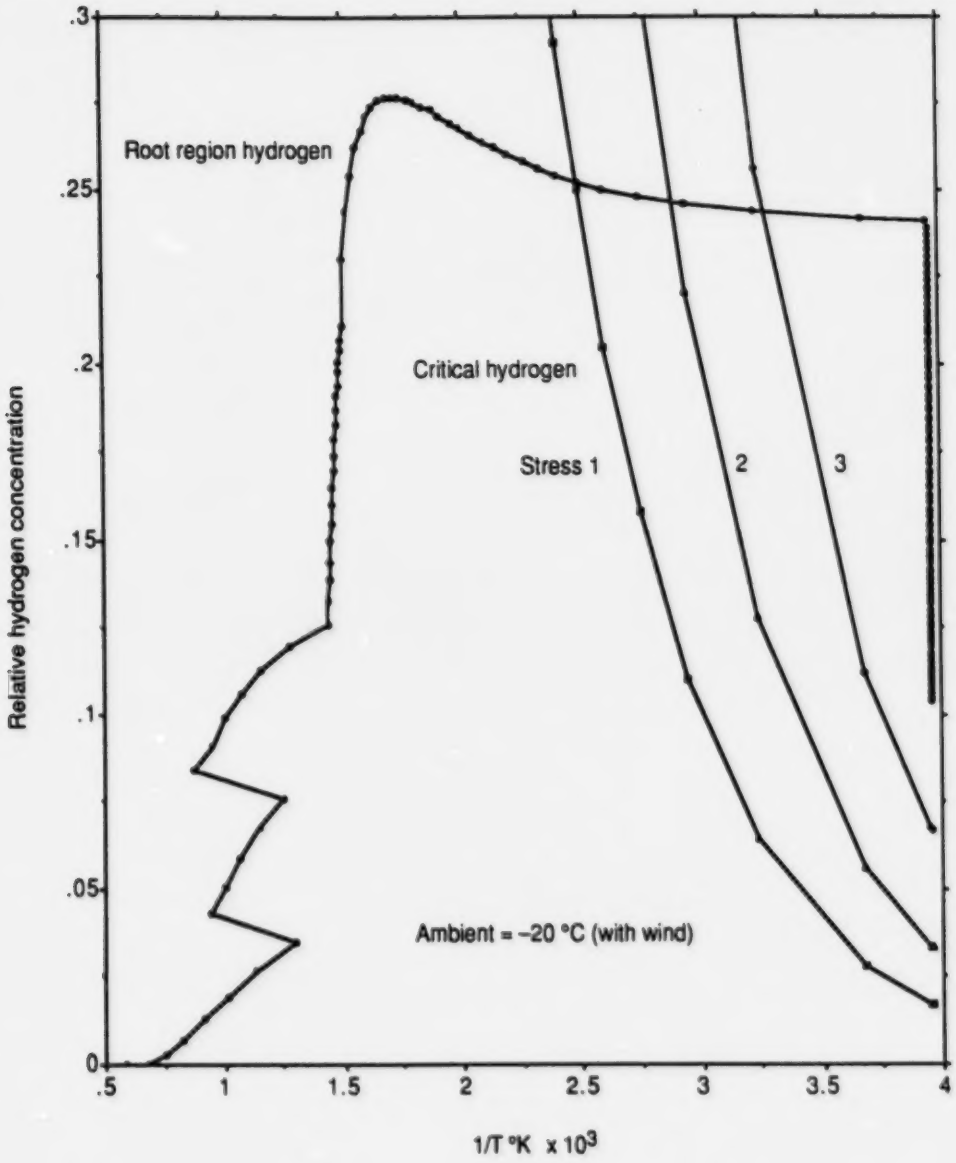

Figure 20. Relative hydrogen concentration against the reciprocal of the absolute temperature for the repair weld at –20 °C with critical hydrogen curves.

HYDROGEN DIFFUSION IN LINE PIPE WELDS

PREPARED BY:

FLEET TECHNOLOGY LTD.
311 LEGGET DRIVE
KANATA, ONTARIO
CANADA
K2K 1Z8

FOR

GRAVILLE ASSOCIATES INC.
P.O. BOX 225
GEORGETOWN, ONTARIO
CANADA
L7G 4Y5

MARCH, 1990

TABLE OF CONTENTS

		Page No.
1.0	Introduction	39
2.0	Geometry	40
3.0	Welding Parameters	40
4.0	Test Matrix	41
5.0	Heat Transfer Coefficient	41
6.0	Finite Element Model	46
7.0	Calculation of Cooling Times and τ	47
8.0	Results and Discussion	48
9.0	Summary	49
10.0	References	50
Tables 1 & 2		51
Table 3		52
Figures 1 to 22		53 to 70

1.0 INTRODUCTION

One of the potential problems that one must guard against in the welding of line pipe is hydrogen-induced cold cracking. Since cold cracks are not acceptable in welds and since they may escape detection and must be repaired if detected, it is essential for the fabricator to take precautions during welding to prevent their initial occurrence.

Cold cracks may occur in the weld metal or in the heat affected zone. During welding, hydrogen is introduced into the molten metal. As the molten metal solidifies and then cools, the resident hydrogen starts diffusing to the HAZ and to the ambient on account of the lower solubility and diffusivity of hydrogen. During this process, and in the presence of susceptible microstructure and stress, if a critical hydrogen concentration is reached, cold cracking will occur.

Whether sufficient hydrogen will diffuse out so that actual hydrogen concentration is below the critical value depends on the environmental conditions (temperature, wind velocity) as well as factors such as the preheat, post-heat, insulation, etc.

The approach has been formalized by Graville whereby

$$\beta \tau_c = 12P_{CM} + \log H_{IIW} + M \qquad (1)$$

In this equation

P_{CM}	=	C+Si/30+Mn/20+Cu/20+Ni/60+Cr/20+Mo/15+V/10+5B
H_{IIW}	=	hydrogen content in ml/100 g of deposited metal (IIW method)
M	=	a factor dependent on the restraint of the weld joint
β	=	a parameter related to the weld size
τ_c	=	diffusion parameter which is indicative of the amount of hydrogen that can diffuse out

Higher the value of τ_c, higher initial hydrogen and/or higher P_{CM} and/or higher restraint can be tolerated without incidence of cold cracking as long as the above equation is satisfied.

τ can be represented as

$$\tau = \int_{50}^{1500} D\Delta t, \qquad (2)$$

where

D = diffusivity of hydrogen as a function of temperature

Δt = the cooling time from 1500°C to 100°C

The above relation is not unique, since 'Δt' is a function of welding and environmental variables, such as heat input, preheat, ambient temperature, wind velocity, etc.

Based on equation (1) above, it is clear that for a given weld joint (weld size, steel composition and restraint fixed)

$$\beta\tau_c = \text{Constant} + \log H_{IIW}$$

i.e. τ_c is linearly related to $\log H_{IIW}$.

Hence, by changing the weld cooling time curves through changes in preheat, heat input, etc., the residual hydrogen content can be reduced and cold cracking can be avoided.

2. GEOMETRY

In the present study, a circumferential four pass girth weld in line pipe is considered. The pipe is 1067 mm (42 in.) in diameter. A longitudinal cross-section through the pipe axis (transverse to the girth weld) shows the joint detail (Figure 1).

3. WELDING PARAMETERS

Table 1 shows the welding parameters selected for the four passes. Since the interpass time in practice is kept within certain limits, both to avoid cold cracking and to maximize productivity, an upper bound value of five minutes for interpass times was chosen between the first three passes. An interpass time of ten minutes between the third and fourth passes was used due to the high heat input of the third pass.

4. TEST MATRIX

As stated before, the cooling time is related to the welding and environmental variables. In order to study these aspects, a test matrix was devised, as shown in Table 2. This comprises eighteen computer runs, nine for the weld thermal histories and the remaining nine for calculating τ values. Specifically, the effect of following variables on cooling time and τ was studied.

a) Preheat (150°, 200°C)
b) Wind velocity (0, 40 km/hr.)
c) Ambient (20, -20°C)
d) Band width (150, 300 mm)
e) Insulation blanket

5. HEAT TRANSFER COEFFICIENT

One of the key input variables in modelling the thermal history is the heat transfer coefficient and changes therein due to the presence of wind, as a function of temperature dependent air properties and changes in ambient temperature. Typical constant values of heat transfer coefficient used for simple weld thermal analysis is 12 w/m^2 °C [1]. However, this value is believed to be valid at lower temperature ranges (≈ 100°C) and static wind conditions. It is known that, at higher temperatures, radiation is the predominant heat loss mechanism and, at lower temperatures, heat carried away by wind is significant.

The heat transfer outside the pipe can have a significant effect on the pipe temperature and on the cooling rate. Therefore, it is essential to have a prediction capability general enough to handle various ambient and wind conditions. Both natural and forced convection must be considered. In addition, radiation needs to be considered.

In the heat transfer correlation used for convection, special consideration must be given to the fact that the heated spot is quite small relative to the pipe size. Therefore, standard correlation may not apply or many have to be modified to account for the starting length of the thermal boundary layer. On the other hand, the flow boundary layer can be assumed to be fully developed. Because of the small area of heating relative to the total area, the temperature rise of the bulk air can be neglected.

A value of the combined convective heat transfer coefficient is calculated for each outside and inside boundary node and is dependent on the inside and outside wall temperature, air properties and the distance from the start of the thermal boundary layer. Inside and outside wall temperatures are computed simultaneously with the heat transfer coefficient by an interactive Newton-Raphson procedure.

The correlations used are based on non-dimensional parameters which include various fluid properties. Thus, they should apply to any fluid so long as it is possible to obtain the required properties for a particular fluid, air in the present case. For the present case, air properties such as Prandtl number, kinematic viscosity, thermal conductivity, density, viscosity, diffusivity, etc. were obtained from literature[2]. These are generally available from 100°K to 3000°K.

The total heat transfer coefficient is the summation of three co-efficient, viz

H_F = Heat transfer coefficient due to forced convection
H_N = Heat transfer coefficient due to natural convection
H_R = Heat transfer coefficient due to radiation

i.e. $H_T = H_F + H_N + H_R$ (3)

For the case when air velocity is zero

$H_T = H_N + H_R$ (4)

In order to apply the convection correlation available in the literature, it is necessary to calculate the non-dimensional Reynold's number. If the Reynold's number (R_e) $\leq 5 \times 10^5$, the flow is laminar.

However, the above value is a representative value. For external flow, it is known to vary from 10^5 to 3×10^6, depending on the surface roughness, the free stream velocity and nature of the pressure variation along the surface.

In case $5 \times 10^5 \leq Re < 10^7$, the flow is in the transition region. Reynold's number $> 10^7$ is in the turbulent region.

For pipes of long length (≈ 100 m), a wind velocity of 11.1 m/s (40 km/hr), and kinematic viscosity of 850×10^{-6} m^2/s,

$$Re = \frac{11.1 \times 100}{850 \times 10^{-6}} = \approx 5.2 \times 10^5$$

Hence, in the present case, the flow is essentially in the laminar region.

Forced Convection Correlation

The equation for fully developed laminar flow[2] is:

$$Nu = 0.664\ Re^{1/2}\ Pr^{1/3} \qquad (5)$$

$$= \frac{hL}{k}$$

$$So,\quad H_F = \frac{0.664\ Re^{1/2}\ Pr^{1/3}\ k}{L} \qquad (6)$$

where Re = Reynold's number = $\frac{UL}{\vartheta}$

Pr = Prandtl number

L = Length (m)

U = Wind Speed (m/s)

ϑ = Kinematic Viscosity (m^2/s)

k = Thermal conductivity (w/m °C)

In this correlation, the temperature dependent properties (viz Pr, ϑ, k) are taken into account by considering the film temperature T_{film}, i.e.

$$T_{film} = \frac{T_{bulk} + T_{wall}}{2}$$

where T_{bulk} refers to the temperature of the wind (ambient) and T_{wall} is the local surface temperature at the inside and outside of the pipe.

This form is most applicable to the current situation where only a small portion of the wall is heated at any one time. This also simplifies the calculation in terms of the variable fluid properties as a function of local node temperature. In the present application, with local heating over a relatively small region, the temperature rise of the bulk fluid is expected to be insignificant and therefore, as an approximation, the temperature rise of the bulk fluid has been neglected.

Equation [6] can be modified by adding a Sider and Tate[3] type viscosity ratio correction factor

$$\frac{\mu_{bulk}}{\mu_{wall}}$$

$$\text{i.e.} \quad H_F = \frac{0.664\ Re^{1/2}\ Pr^{1/3}\ k \left(\frac{\mu_{bulk}}{\mu_{wall}}\right)^{.25}}{L}$$

In this equation, all properties are evaluated at the μ_{bulk} fluid temperature, except the μ_{wall} term in the viscosity ratio term which is evaluated at the local wall temperature.

Natural Convection Correlation

The importance of natural convection (free convection) compared to forced convection can be firmly judged by the relevant dimensionless parameter, namely Reynold's number (Re) and Grashof number (Gr), i.e.

$$\text{If } \frac{Gr}{Re^2} >> 1 \text{ "Pure" free convection}$$

$$\frac{Gr}{Re^2} \approx 1 \text{ Mixed convection}$$

$$\frac{Gr}{Re^2} << 1 \text{ "Pure" forced convection}$$

A quick check (under 40 km/hr wind velocity) indicates that this ratio is much smaller than 1 in the present case, and the effect of free convection compared to forced convection or radiation will be small.

For free or natural convection, the following equation has been used[3]

$$H_N = \frac{0.508\ Pr^{.25}\ R_A^{.25}}{(.952 + Pr)^{.25}} \frac{k}{L}$$

$$\text{where } R_A = \frac{\beta G\ (T_{wall} - T_{Bulk})\ L^3}{Nu\ \alpha}$$

Nu = Nusself Number
α = thermal diffusivity
G = acceleration due to gravity = 1.0 for horizontal plate

Radiation Heat Transfer Coefficient

For radiation, the following relationship has been used[4]:

$H_{Rad} = 0.00216 (T_{wall} - T_{Bulk})^{1.61}$

T_{wall} is the temperature of inside and outside surface nodes.

6. FINITE ELEMENT MODEL

A longitudinal cross-section of the pipe was considered for finite element modelling. Due to symmetry, only one half of the cross-section was considered. (Figure 2). The individual weld passes were modelled as double ellipsoidal heat source[5]. The relevant fusion area, reinforcement area, bead height, width, penetration was obtained from the literature[6] corresponding to the heat inputs of 1.1, 1.2, 2.0 and 3.0 kJ/mm respectively. Temperature dependent thermal properties for heat flow calculation were obtained from BISRA handbook[7].

A total of nine welds, each with four passes, were simulated as per the test matrix (Table 2). The heat transfer coefficients were obtained as discussed in Section 5. Wind velocity of 0.5 m/s was assumed to be present at all times at inside diameter and at outside diameter when static wind velocity was to be modelled.

At the end of the elapsed time for a particular pass, the next pass was deposited. This sequence was maintained until the end of the fourth pass. From then on, the weld was allowed to cool down to about 50°C.

7. CALCULATION OF COOLING TIMES AND τ

Figure 3 shows a schematic of the weld joint with four pass weld deposited into the groove. The point 'A' is the root pass toe location at I.D. surface and 'B' is the capping pass toe location at the O.D. These are the two locations of primary interest in the current program.

For calculation of $\tau = \int_{50}^{1500} D\Delta t$ (equation 2), the cooling curves for location 'A' due to all the four passes and location 'B' due to the 4th pass was numerically integrated between the appropriate limits to obtain τ from 1500° to 50°C.

The temperature dependent diffusivities were obtained from the following relationship[8]

$$D(cm^2) = 4.3 \times 10^{-2} \exp\left(\frac{-3358}{T}\right) \quad \text{for } T \leq 423°K$$

$$= 2.4 \times 10^{-3} \exp\left(\frac{-2132}{T}\right) \quad \text{for } 423°K < T \leq 773°K$$

$$= 7.1 \times 10^{-4} \exp\left(\frac{-4555}{T}\right) \quad \text{for } T > 773°K$$

The cooling times from 1500 - 100°C and 1500° - 50°C as defined in Figure 4 were also obtained from these curves. Figures 5 to 13 show, for the 9 welds, the temperature history at point 'A' due to all the four passes.

The cooling times from 800 - 500° were also calculated from thermal history curves.

8. RESULTS AND DISCUSSION

Table 3 shows the summary of the results obtained. Figures 14 to 17 show the cooling times between 1500-100°C (S1500-100) and 1500-50°C (S1500-50) as a function of τ. As can be seen, τ is approximately proportional to S1500-100 and S1500-50.

8.1 Effect of Wind Velocity on τ

Figure 18 shows the effect of changes in wind velocity from 0 km/hr to 40 km/hr on τ At the inside of the pipe (point 'A'), there is a decrease of 20% in τ value, and at the outside (point 'B'), τ decreases by 29%. Under lower ambient temperature (-20°C), the changes are 32% and 44%, respectively.

Thus, τ decreases with increasing wind velocity.

8.2 Effect of Ambient Temperature on τ

Figure 19 shows the effect of changes in ambient temperature from 20°C to -20° on τ. At the inside of the pipe (point 'A'), there is an increase of 7%, and at the outside (point 'B'), there is an increase of 12%. Under increased wind velocity (40 km/hr), the changes are 20% and 33%, respectively.

Thus, τ increases with increasing ambient temperature.

8.3 Effect of Preheat on τ

Figure 20 shows the effect of changes in preheat temperature from 150°C to 200°C. Under 'no wind', -20°C ambient temperature conditions, τ changes by 3% at the inside diameter of the pipe.

Thus, τ increases with increasing preheat levels.

8.4 Effect of Band Width on τ

Figure 21 shows the effect of increasing the length of the preheated band on τ. As the length of the bandwidth is increased from 150 mm to 300 mm. τ increases by 6% at the I.D. and by 13% at the O.D.

Thus, τ increases with increasing length of band width.

8.5 Effect of Insulation on τ

Figure 22 shows the effect of providing insulation blankets after the completion of the first pass and/or the last pass, at -20°C ambient temperatures, both in the presence and absence of wind.

Compared to no insulation and zero wind, τ increases by 10% where insulation is provided after first pass, and by 2% when insulation is provided after last pass. In the presence of wind, however, insulation blankets after the last pass increase τ value by ≈ 30%

9.0 SUMMARY

The effect of several variables on τ values has been estimated for a four-pass girth weld and it was found that:

τ decreases with increasing wind velocity;

τ increases with increasing ambient temperature;

τ increases with increasing preheat;

τ increases with increasing band width;

τ increases when insulation blanket is provided.

For the various values used, wind velocity and ambient temperature had significant effects on τ values; the increases in preheat (150°C to 200°C) and preheat bandwidth (150 m to 300 m) had smaller effects.

Going back to equation (1), it is clear that when P_{CM}, M and β are constant, if τ_c (critical diffusion parameter) is decreased by say 10%, there will be a larger decrease in hydrogen content (H_{IIW}) required in order that cracking may not occur.

10. REFERENCES

1. Friedman, E., "Thermomechanical Analysis of the Welding Process using the Finite Element Method." Trans. ASME, August 1975, pp 206.

2. Incropera, Frank P. and Dewitt, David P., "Fundamentals of Heat Transfer."

3. Eckert, E.R.G. and Drake, Robert M. Jr., "Analysis of Heat and Mass Transfer."

4. Vinokurov, V.A., "Welding Stresses and Distortion," The British Library, Lending Division, Translated from Russian into English by J.E. Baker.

5. Goldak, J.A., Chakravarti, A.P., Bibby, M.J., "A New Finite Element Model for Welding Heat Sources," Met. Trans. B, 15B, June 1984.

6. Clark, J.N., "Manual Metal Arc Weld Modelling - Part 1 - Effect of Process Parameters on Dimensions of Weld Bead and Heat-Affected Zone," Materials Science and Technology, December 1985, Vol. 1.

7. The British IRON and STEEL Research Association, "Physical Constants of Some Commercial Steels at Elevated Temperatures," London Butterworths Scientific Publication, 1953.

8. Sakai, T., Asami, K., Katsumata, M., Takada, H., Tanaka, O., "Hydrogen Induced Disbonding of Weld Overlay in Pressure Vessels and Its Prevention".

Table 1

Welding Parameters

Pass No.	Current (amp)	Voltage (volts)	Speed (mm/s)	Heat Input (KJ/mm)	Time for Completion of Pass (m/s)
1	137	26	3.0	1.2	5
2	142	28	3.6	1.1	5
3	155	28	1.5	3.0	10
4	155	28	2.1	2.0	-

Table 2

Test Matrix

	Run No.								
	1	2	3	4	5	6	7	8	9
Thickness, mm	10	10	10	10	10	10	10	10	10
Preheat, 0°C	150	150	150	150	150	150	200	150	150
Band width, mm	150	150	150	150	150	300	150	150	150
Ambient, °C	20	20	-20	-20	-20	-20	-20	-20	-20
Wind, km/hr	40	0	40	0	0	0	0	0	40
Insulation	-	-	-	-	After last pass	-	-	After first pass	After last pass

Table 3
Cooling Times and τ Values

Run No.	I.D. SURFACE S1500–100 (s)	I.D. SURFACE S1500–50 (s)	I.D. SURFACE S800–500* (s)	O.D. SURFACE S1500–100 (s)	O.D. SURFACE S1500–50 (s)	O.D. SURFACE S800–500** (s)	τ(cm²0) to 50°C I.D. (Point A)	τ(cm²0) to 50°C I.D. (Point B)	Conditions
1.	1989.84	3000.33	14.04	741.47	1495.12	26.09	6.97E–2	2.61E–2	20°C Wind 40 km/hr
2.	2390.54	4500.61	15.01	1072.33(1700)	2614.11	27.00	8.77E-2	3.67E-2	20°C No Wind
3.	1748.24	2232.69	14.34	500.86(800)	985.04	25.81	5.52E-2	1.73E-2	-20°C Wind 40 km/hr
4.	2204.14	3603.30	13.99	906.87	2050.00	29.17	8.15E-2	3.13E-2	-20°C No Wind
5.	2268.17	3805.10	13.99	957.58	2356.03	31.41	8.34E-2	3.44E-2	-20°C No wind Insulation after last pass.
6.	2370.74	4245.92	13.98	1026.69	2561.05	28.89	8.65E-2	3.59E-2	-20°C Band width 300mm No Wind
7.	2272.83	3805.10	17.36	1021.57	2490.56	32.39	8.37E-2	3.52E-2	-20°C Preheat 200°C No Wind
8.	2500.02	4900.79	14.39	1127.12	2999.15	32.66	8.96E-2	3.88E-2	-20°C No Wind Insulation after 1st pass
9.	2108.83	3245.97	-	860.93	1995.71	-	7.3E-2	3.01E-2	-20°C Wind 40 km/hr Insulation after pass

* S800-500 due to 1st pass at the I.D. of the pipe.
**S800-500 due to 4th pass at the O.D. of the pipe;

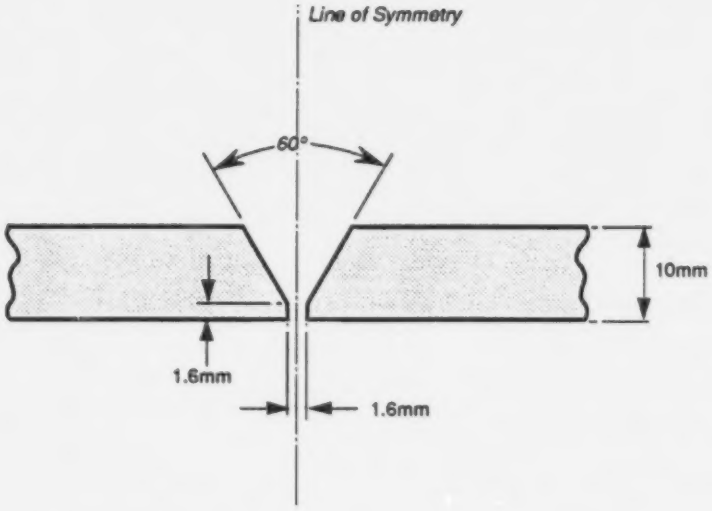

Figure 1 Weld Joint Details

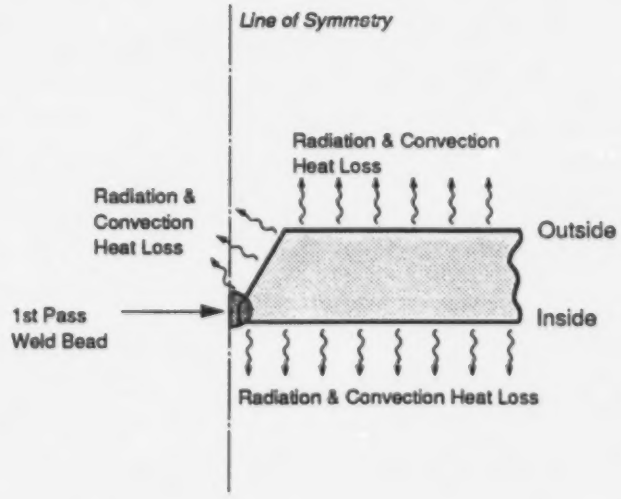

Figure 2 Boundary Conditions for Thermal Analysis

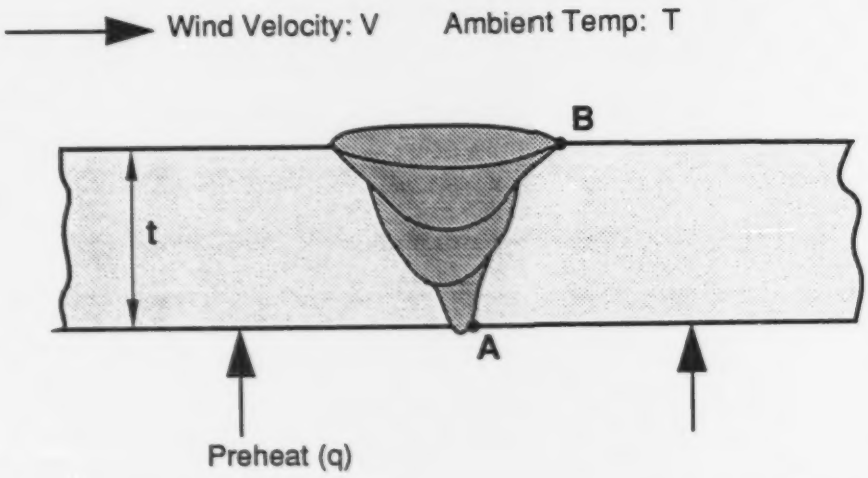

Figure 3 Schematic of Weld Joint

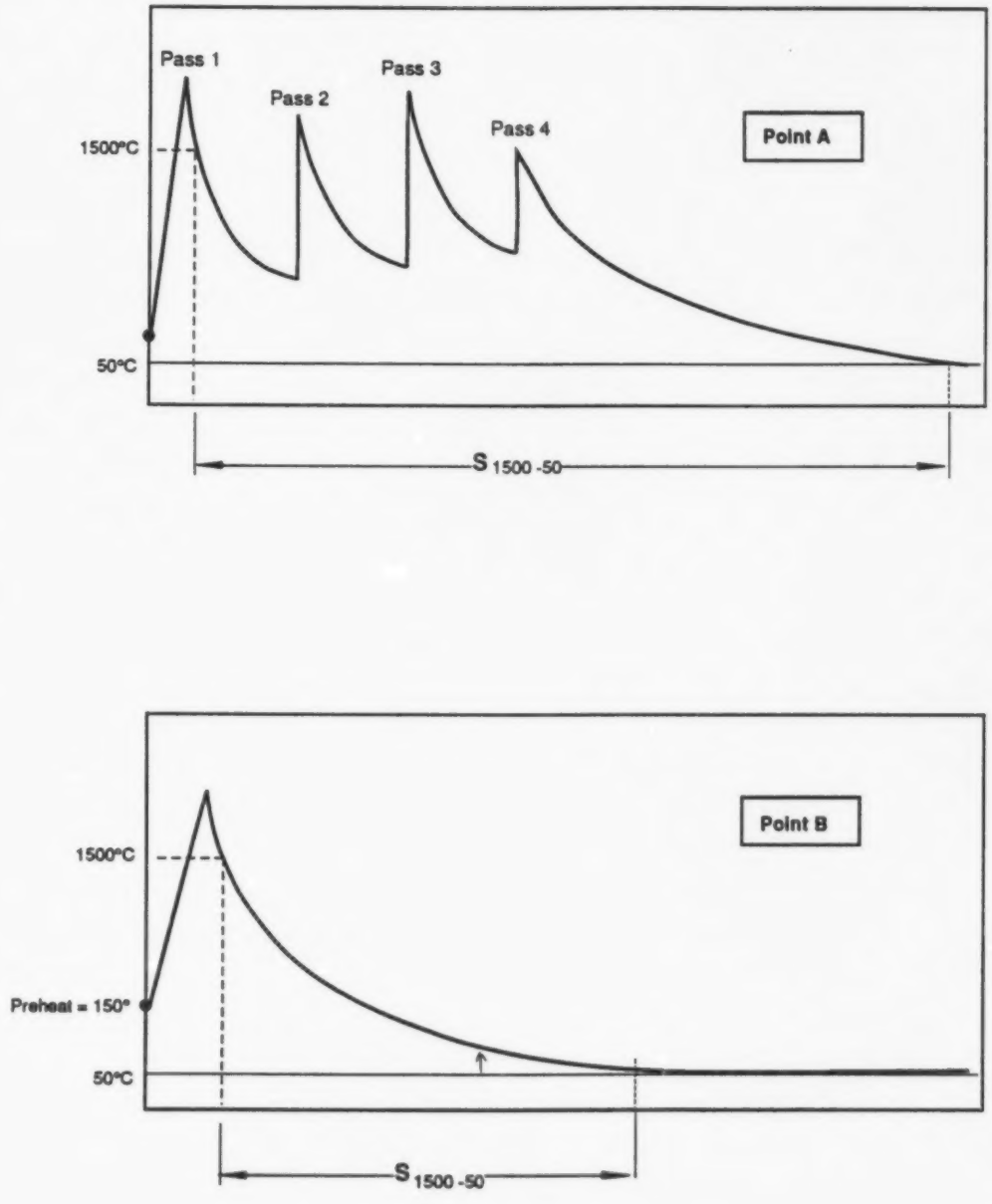

Figure 4 Schematic Thermal History of Weld at Point A and Point B

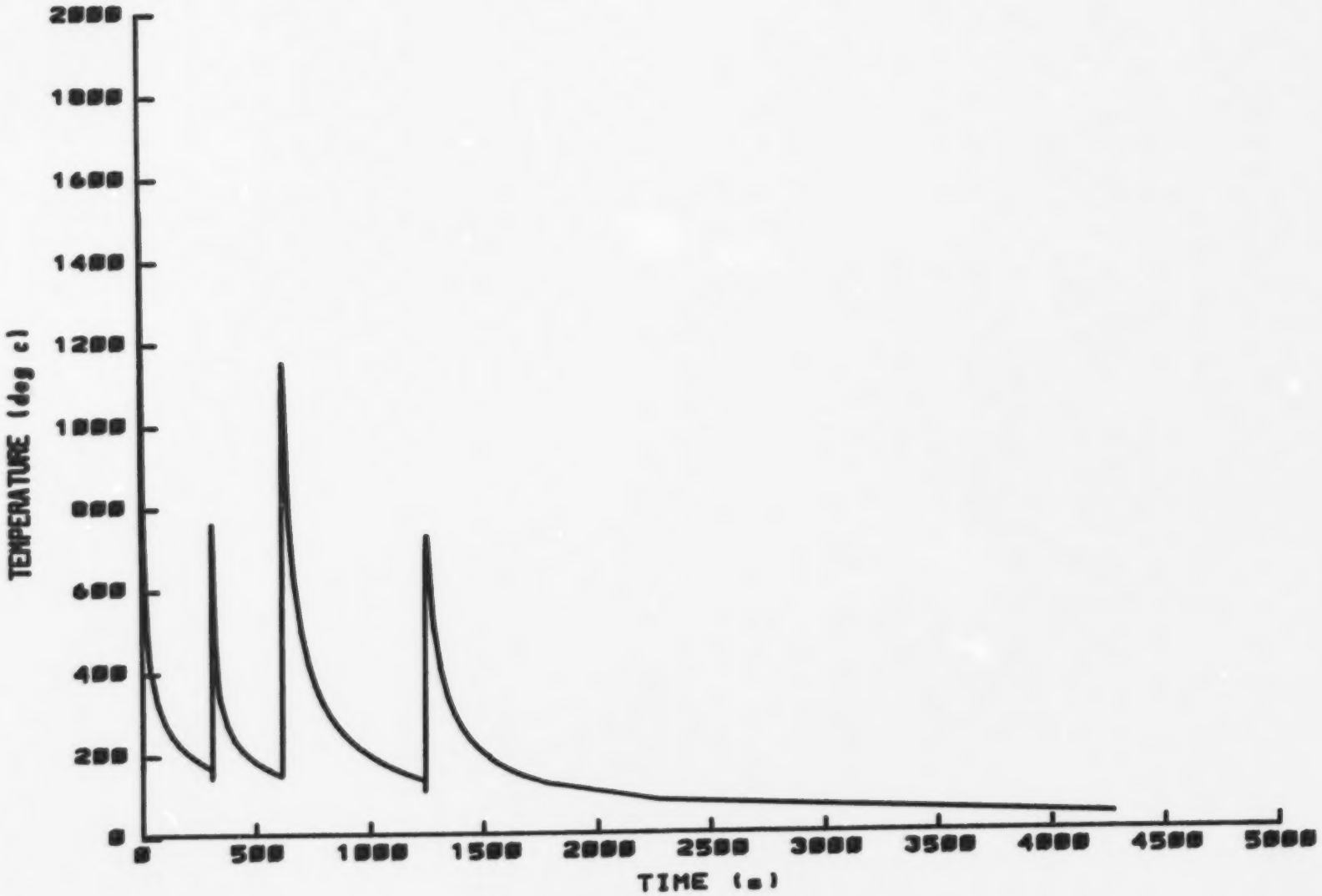

Figure 5: AMBIENT = 20 DEG C. WIND = 40 KM/HR.

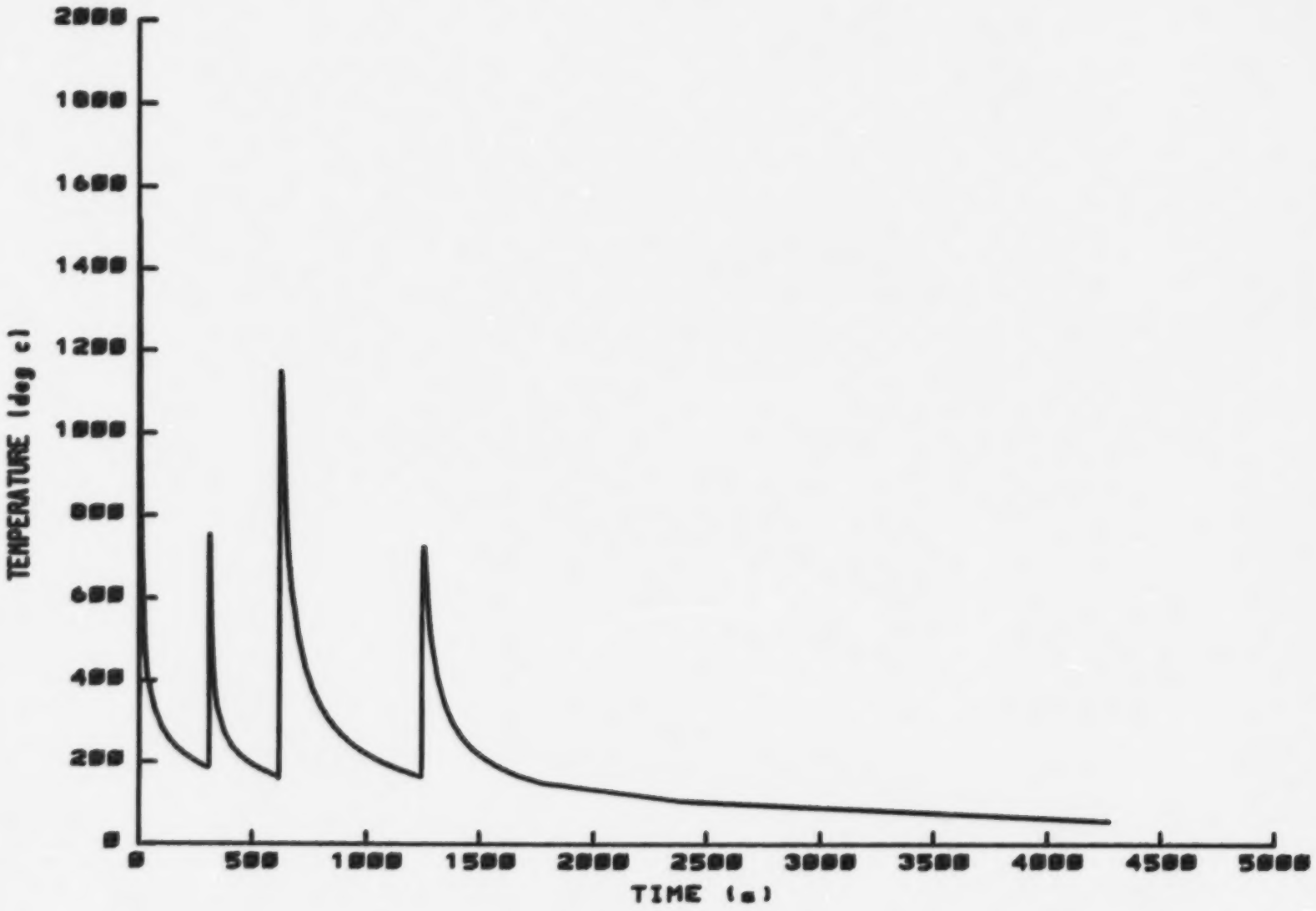

Figure 6: AMBIENT = 20 DEG C. WIND = 0.0.

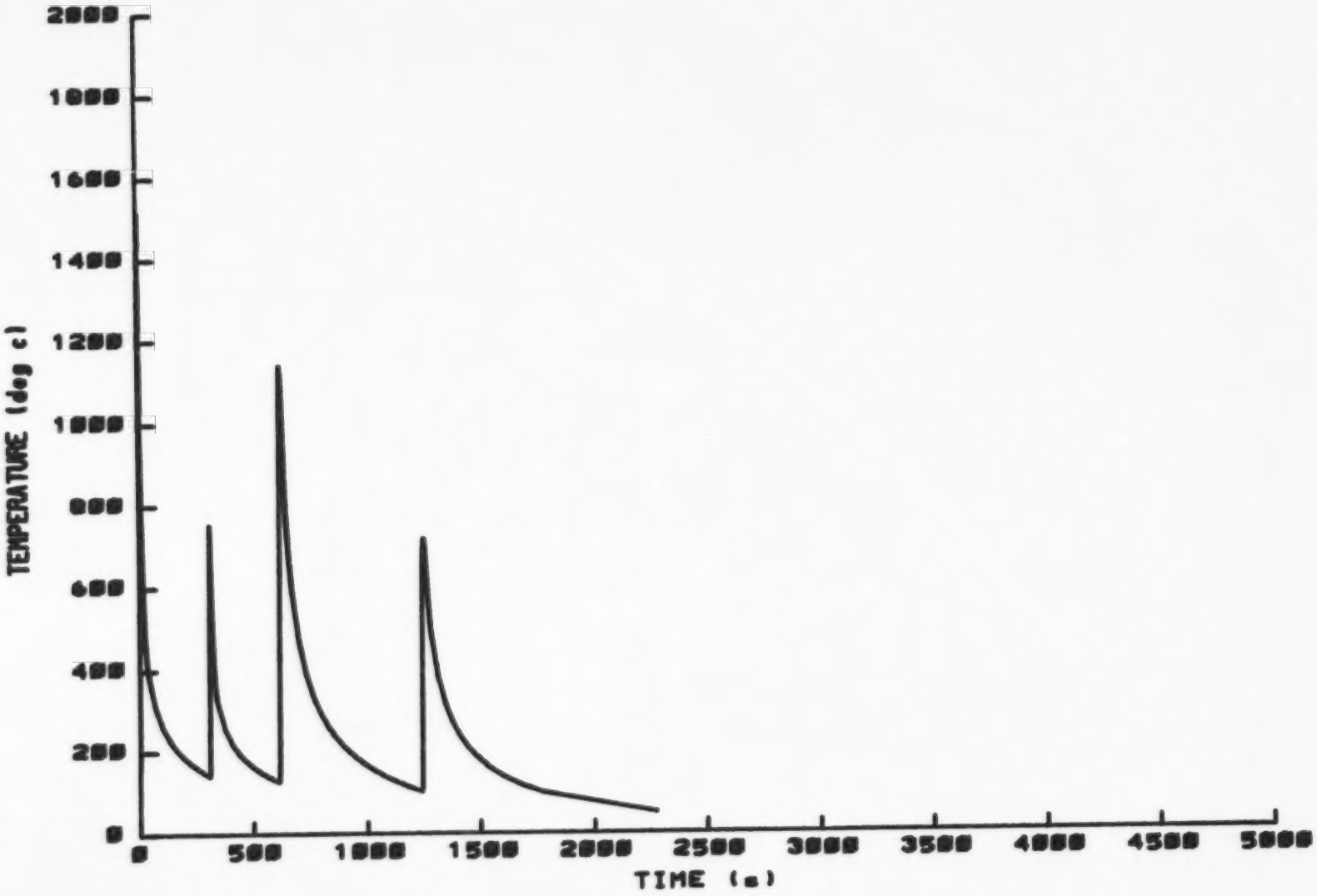

Figure 7: AMBIENT = -20 DEG C. WIND = 40 KM/HR.

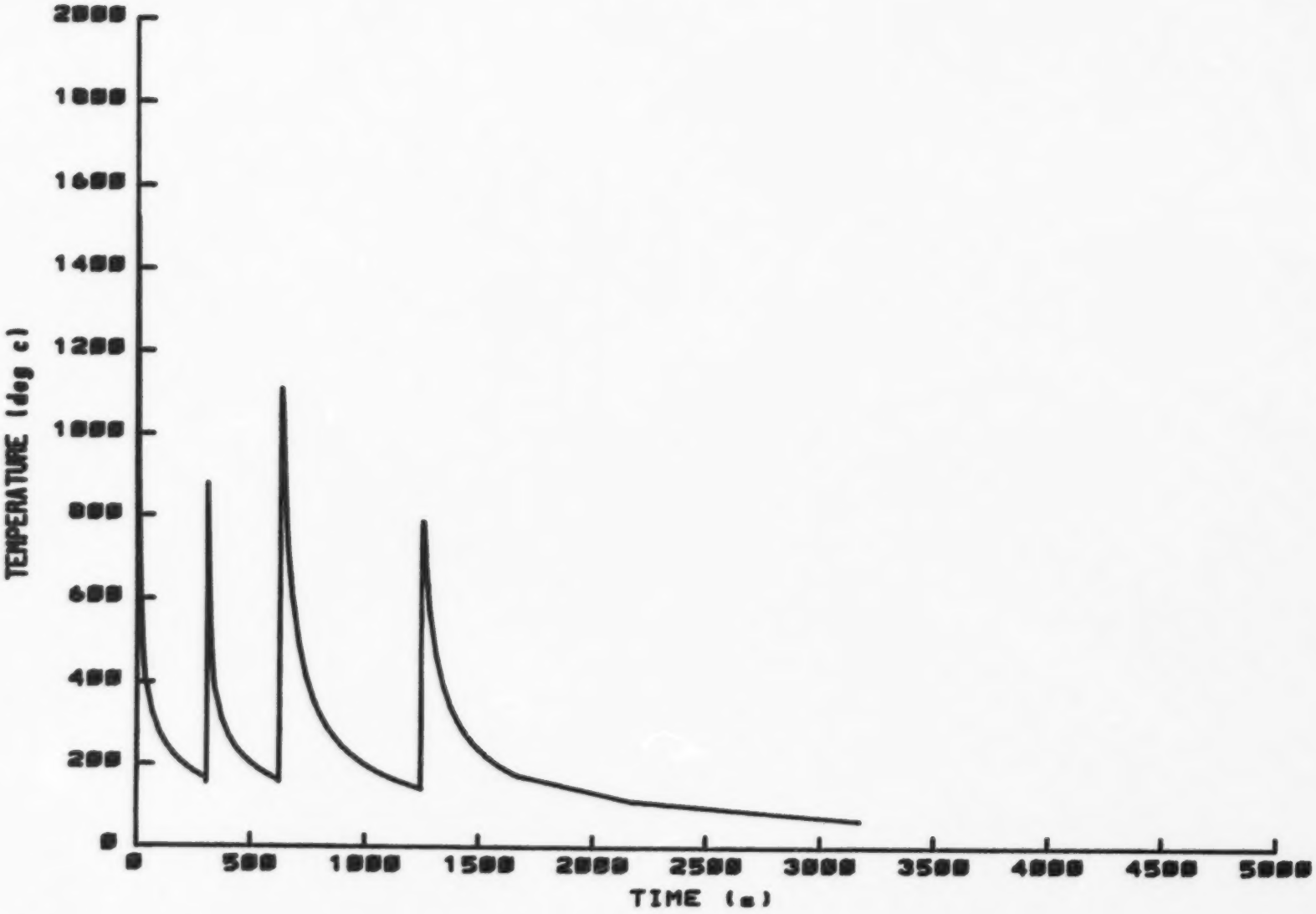

Figure 8: AMBIENT = -20 DEG C. WIND = 0.0.

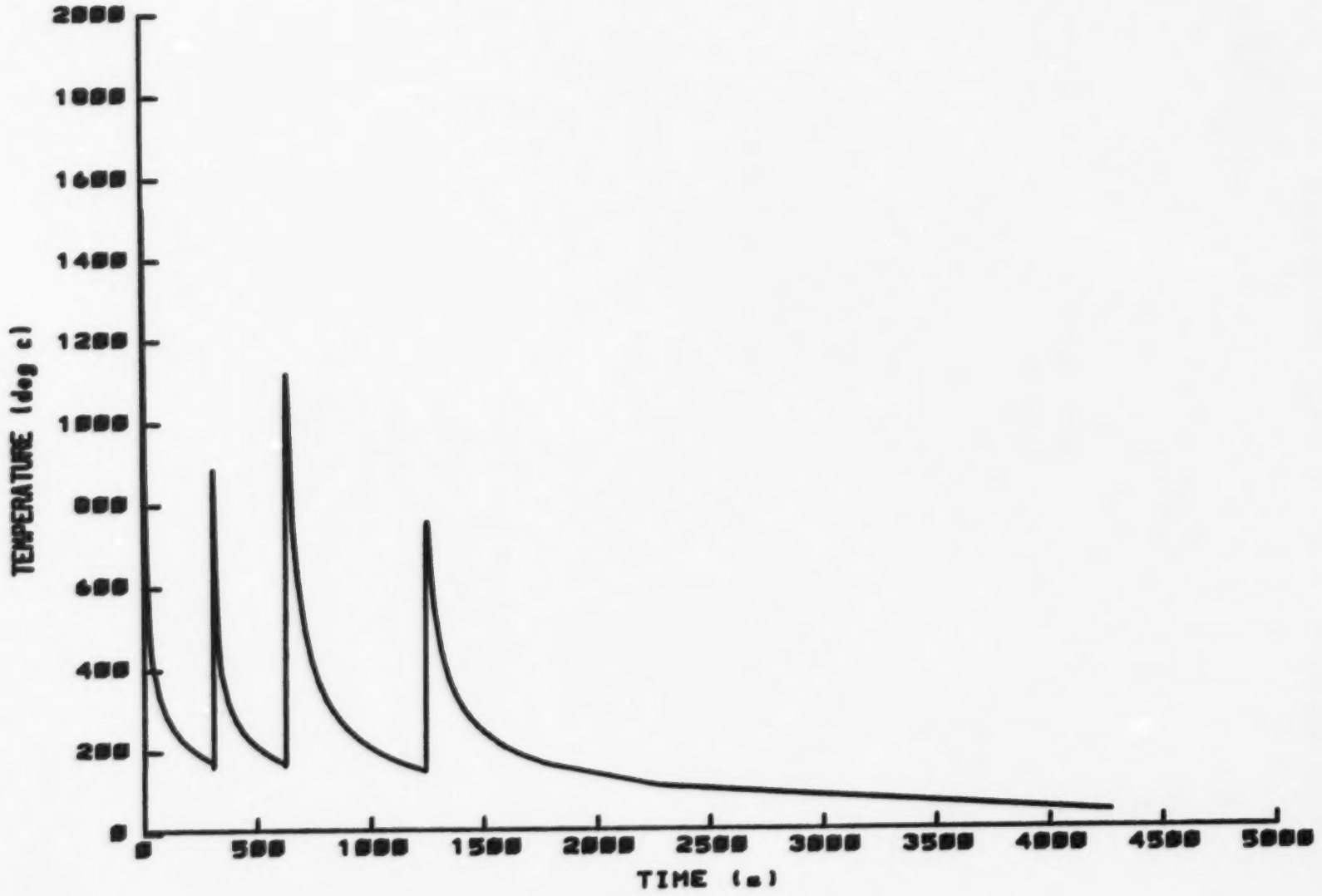

Figure 9: AMBIENT = -20 DEG C. WIND =0.0. INSULATIØN AFTER PASS 4.

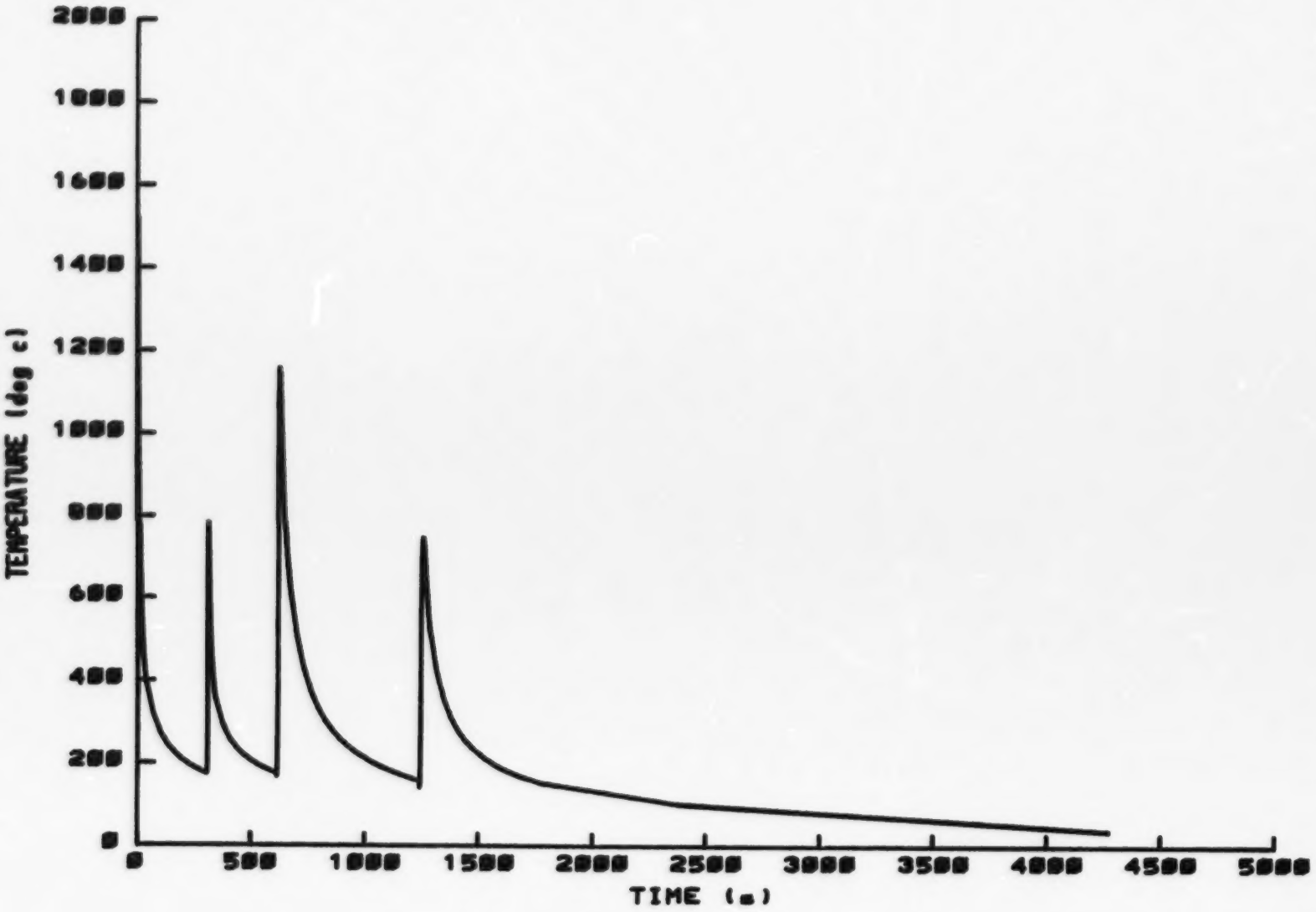

Figure 10: AMBIENT = -20 DEG C.WIND = 0.0. BANDWIDTH = 300 MM.

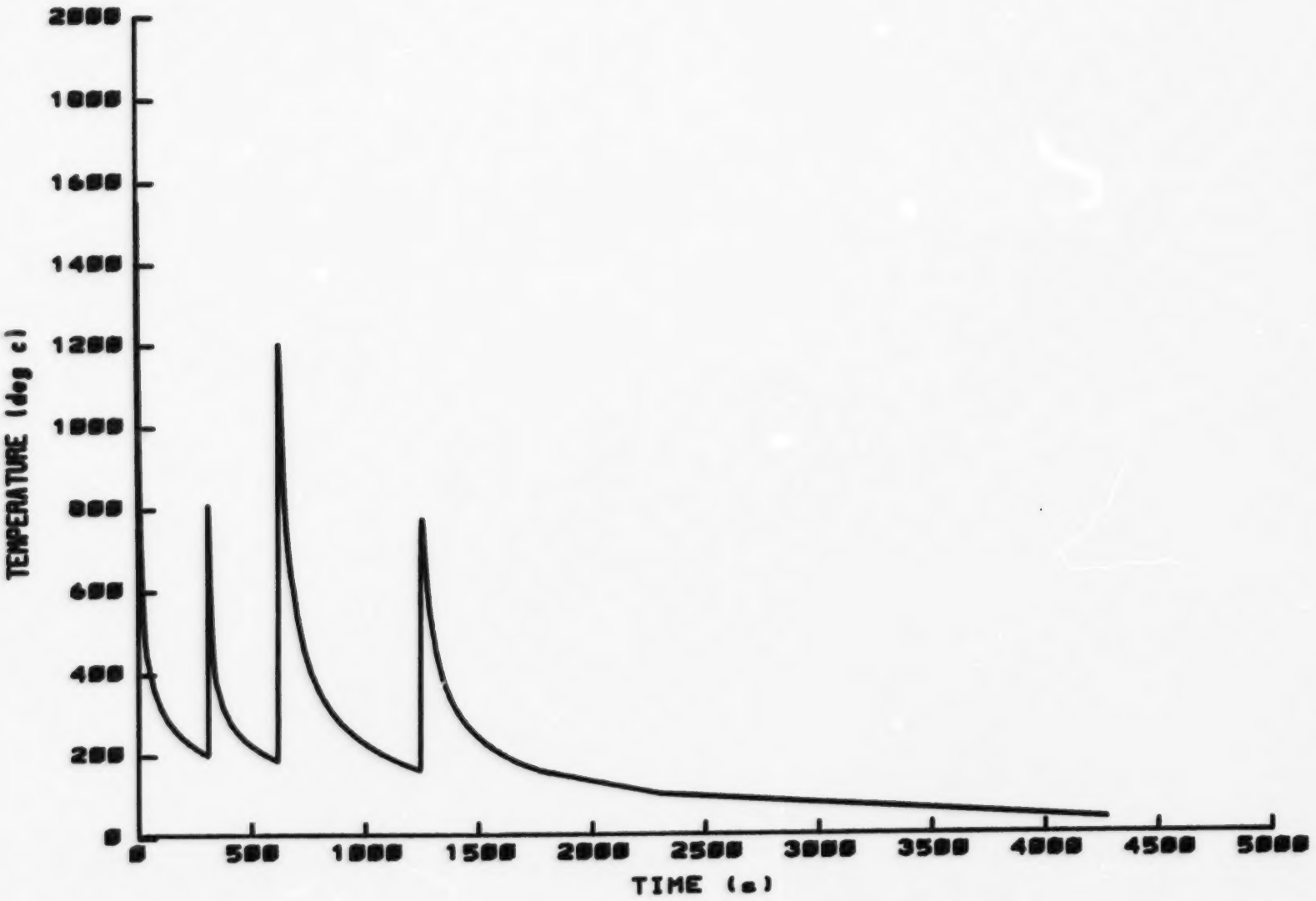

Figure 11: AMBIENT = -20 DEG C.WIND = 0.0. PREHEAT = 200 DEG C.

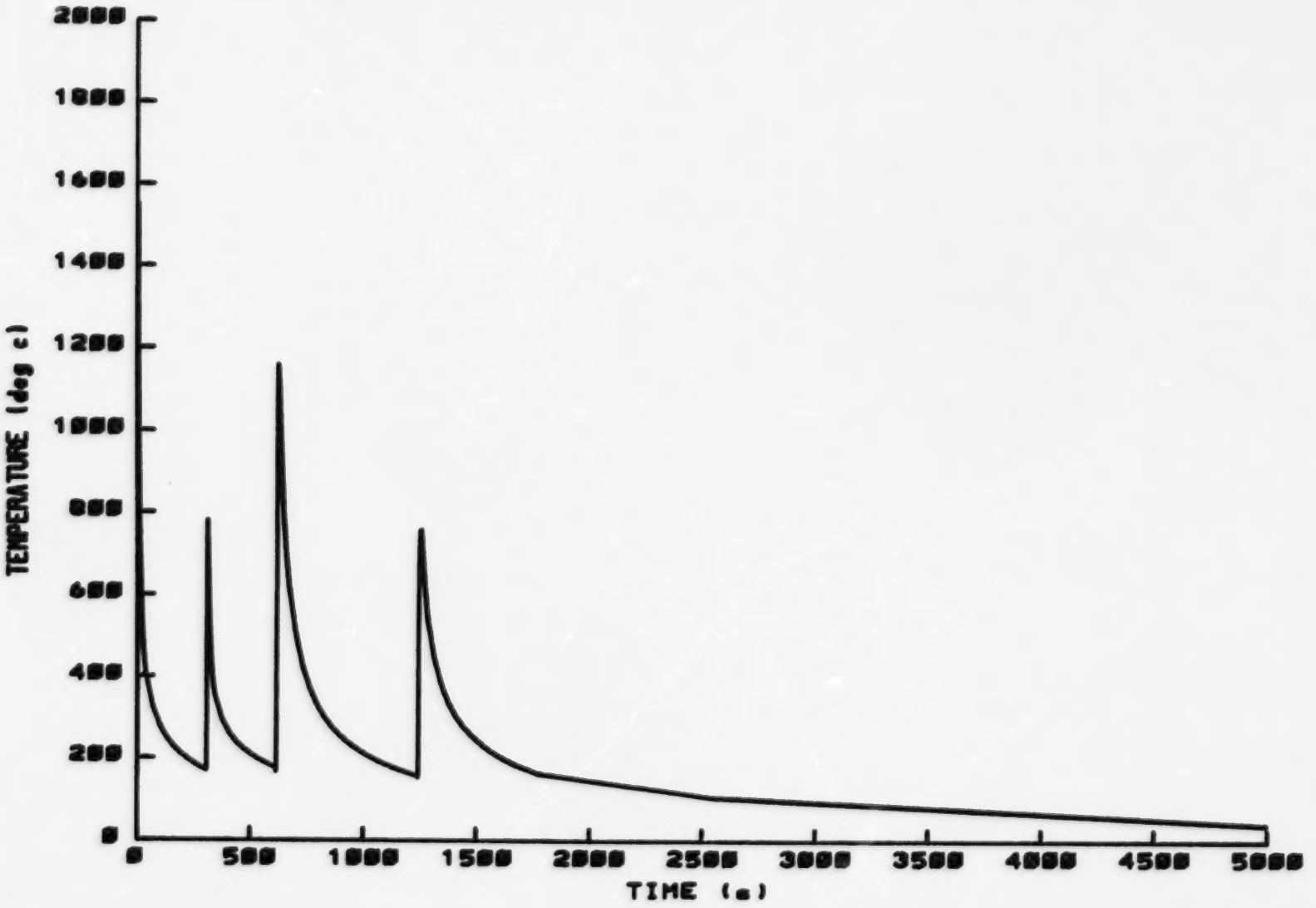

Figure 12: AMBIENT = -20 DEG C.WIND = 0.0.INSULATIØN AFTER PASS 1.

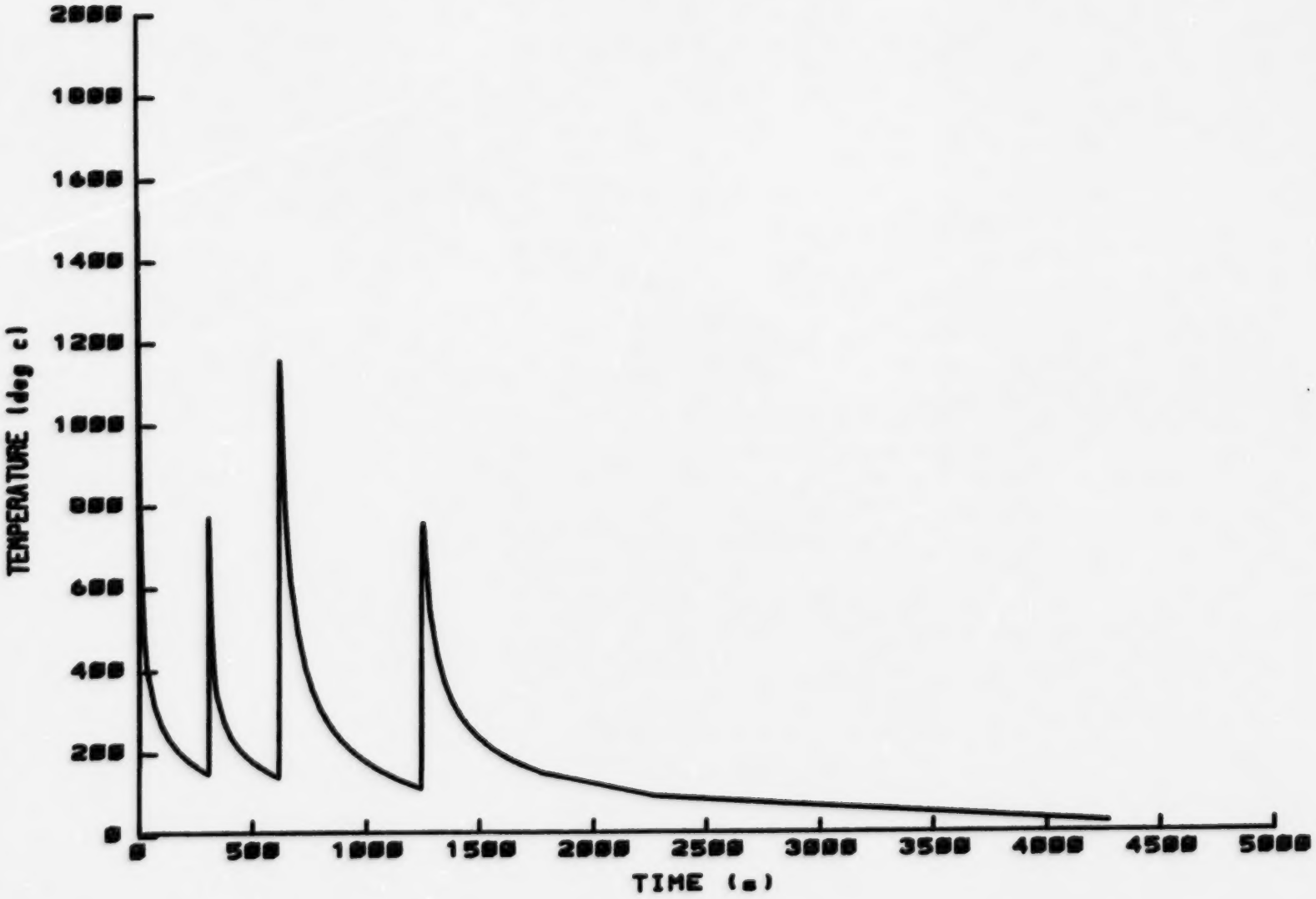

Figure 13: AMBT.=-20 DEG C.WIND=40 KM/HR. INSULATIØN AFTER PASS 4.

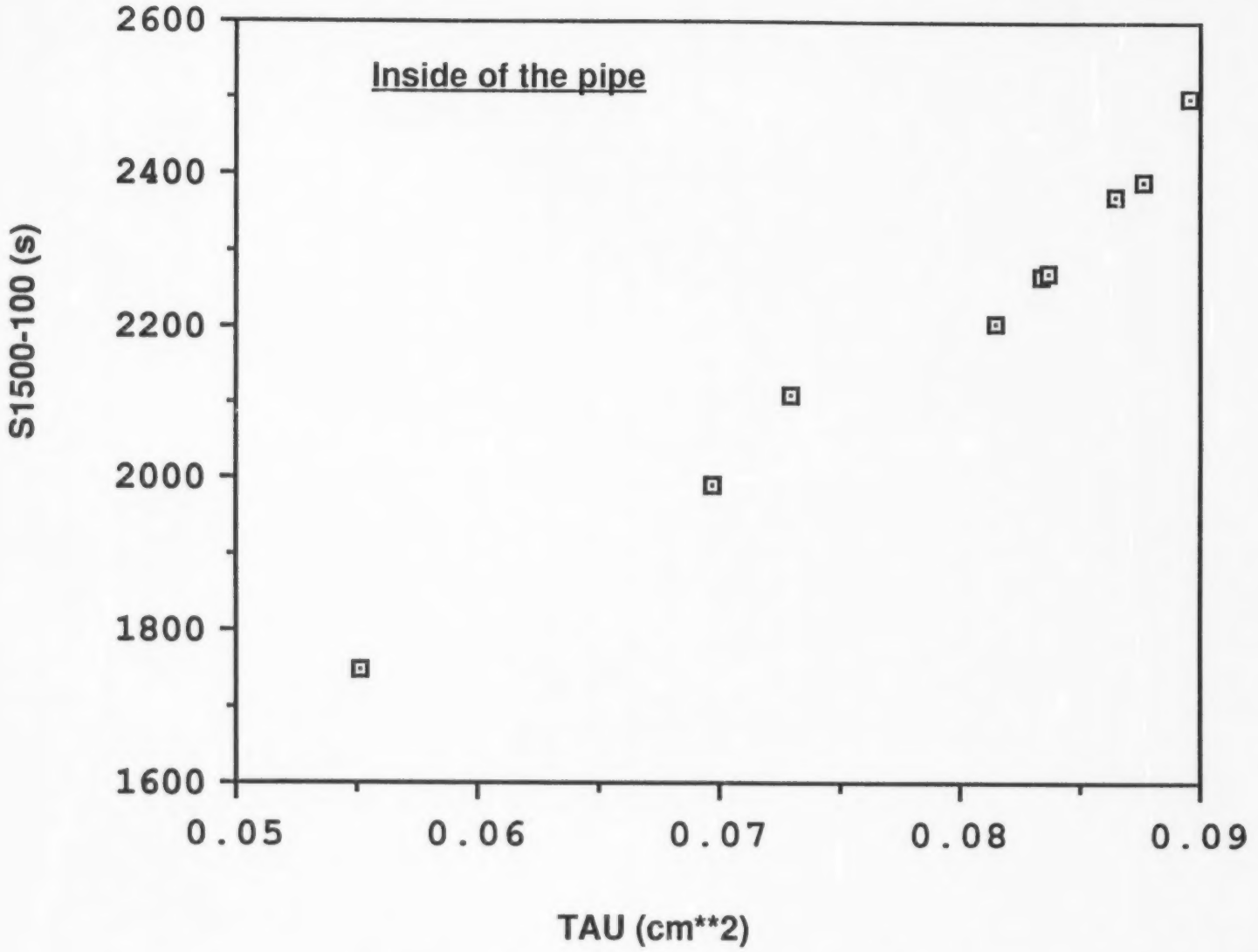

Figure No. 14: Plot of S1500-100 Vs. Tau.

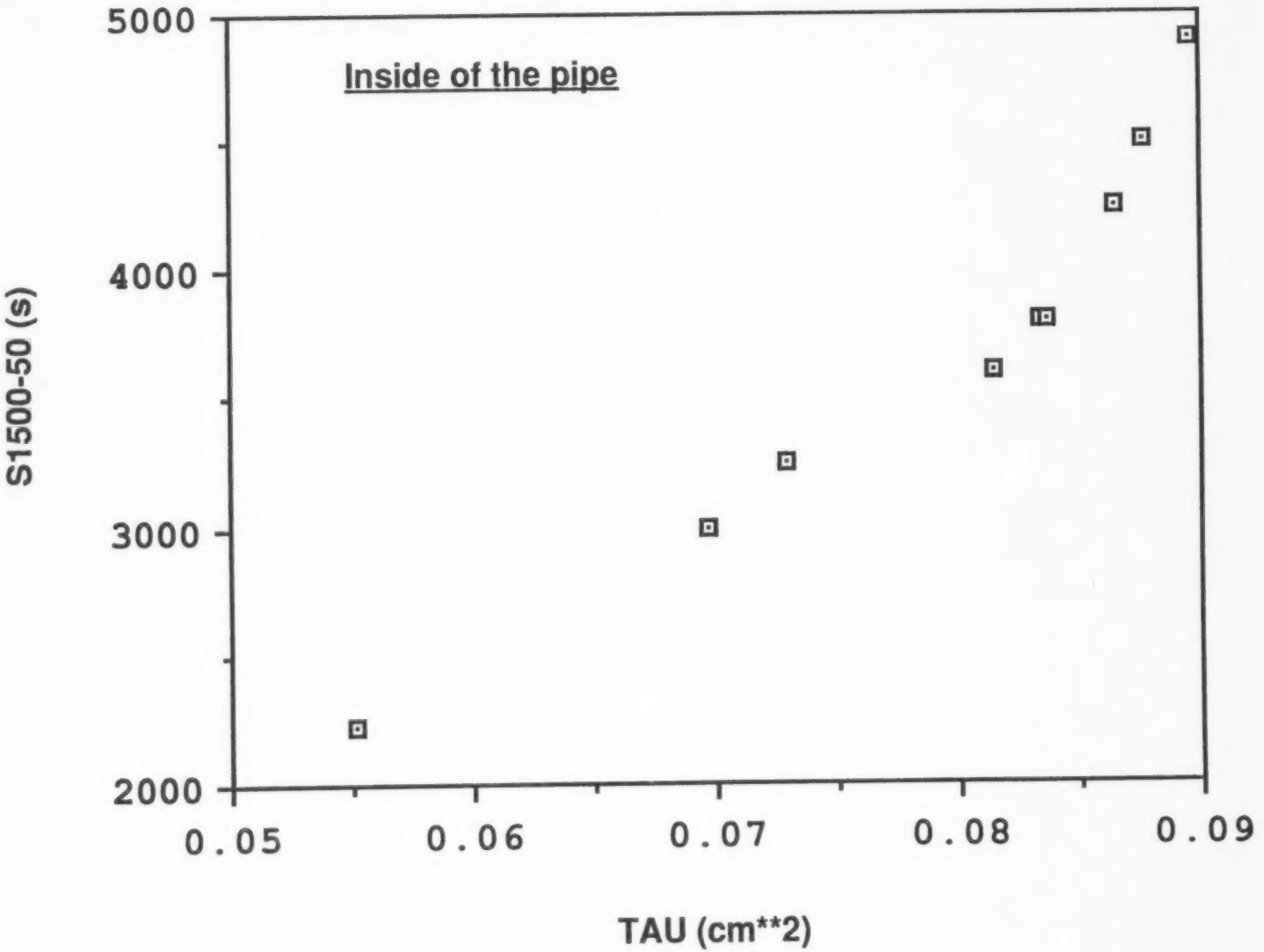

Figure No. 15: Plot of S1500-50 Vs. Tau.

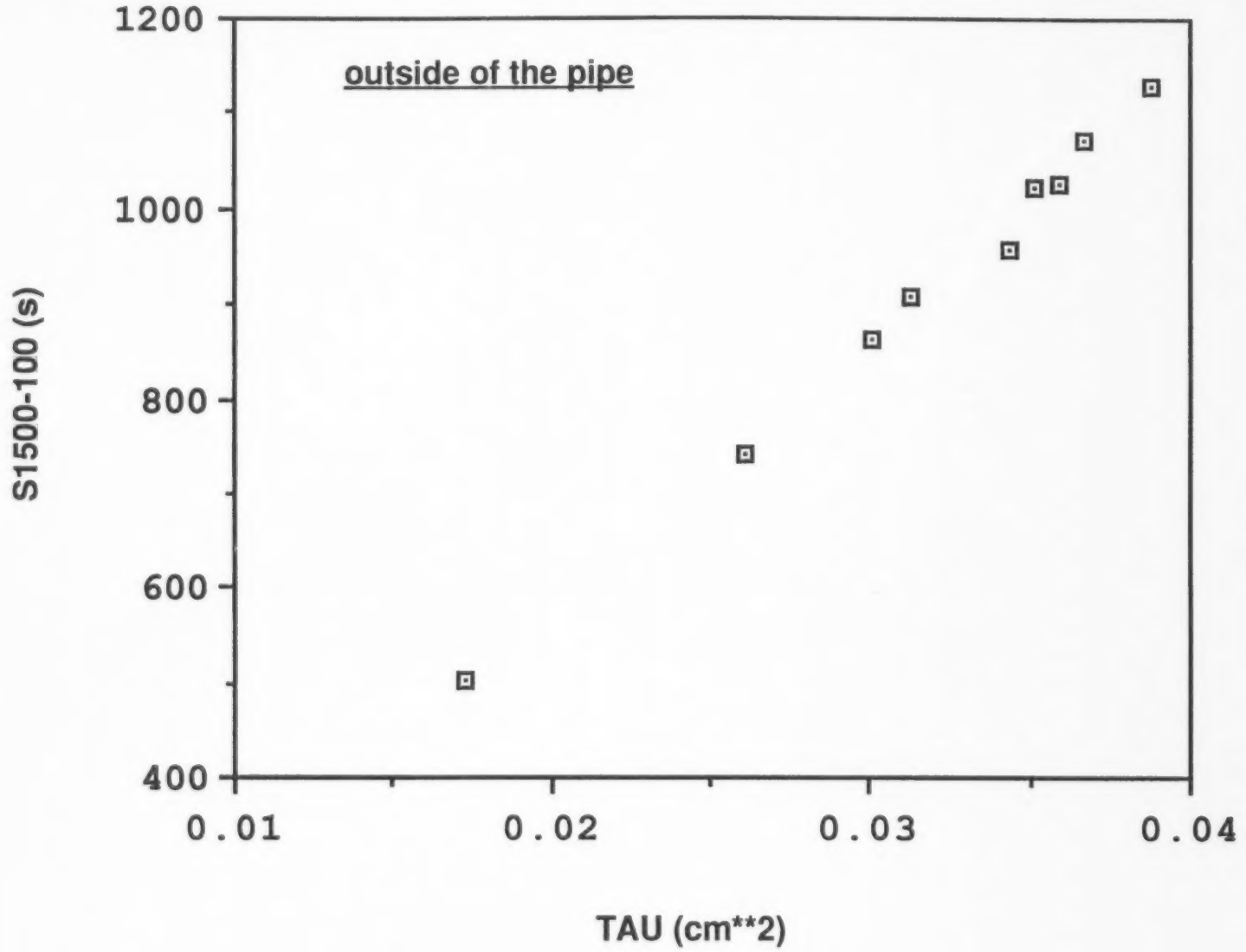

Figure No. 16: Plot of S1500-100 Vs. Tau.

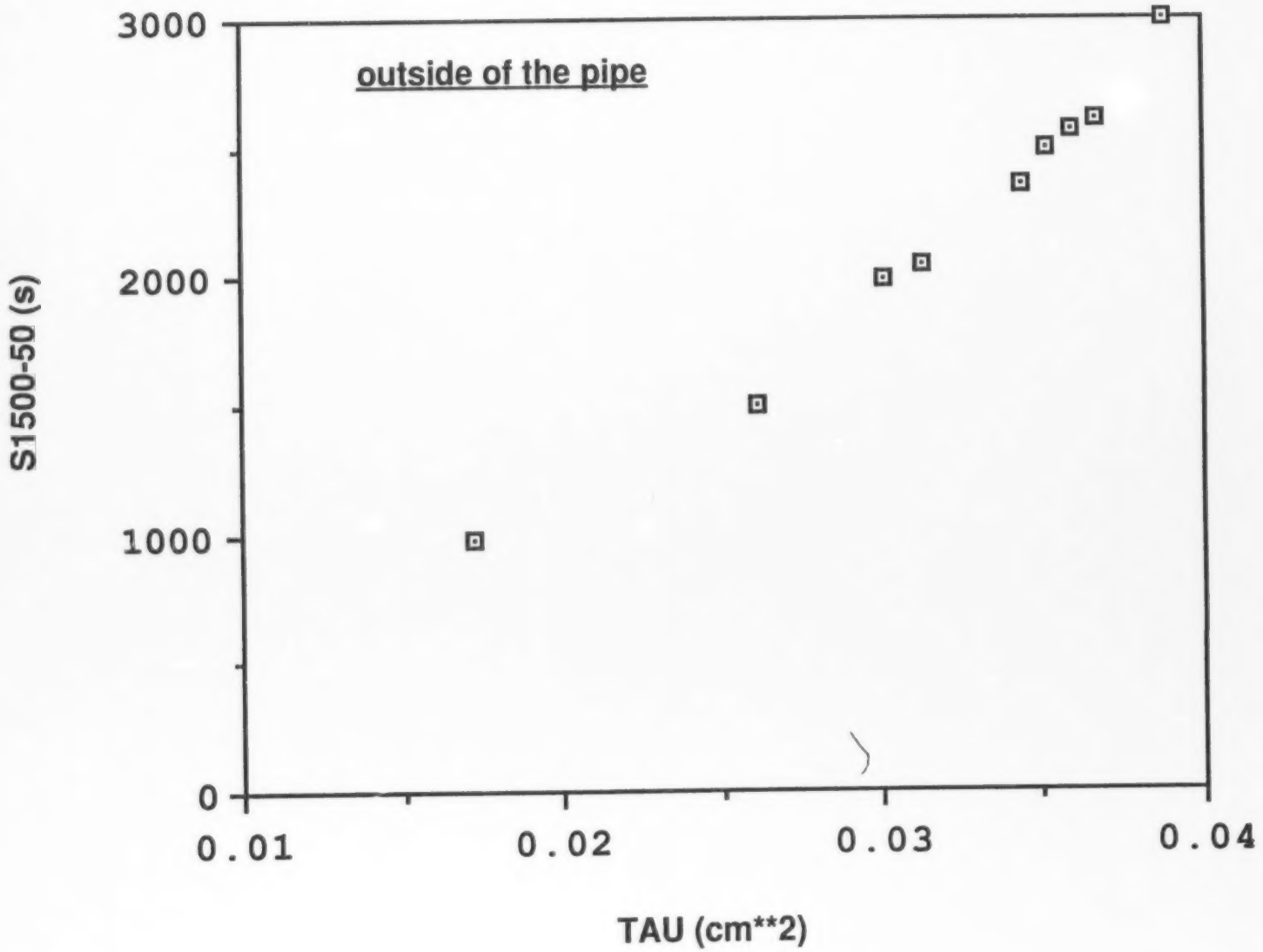

Figure No. 17: Plot of S1500-50 Vs. Tau.

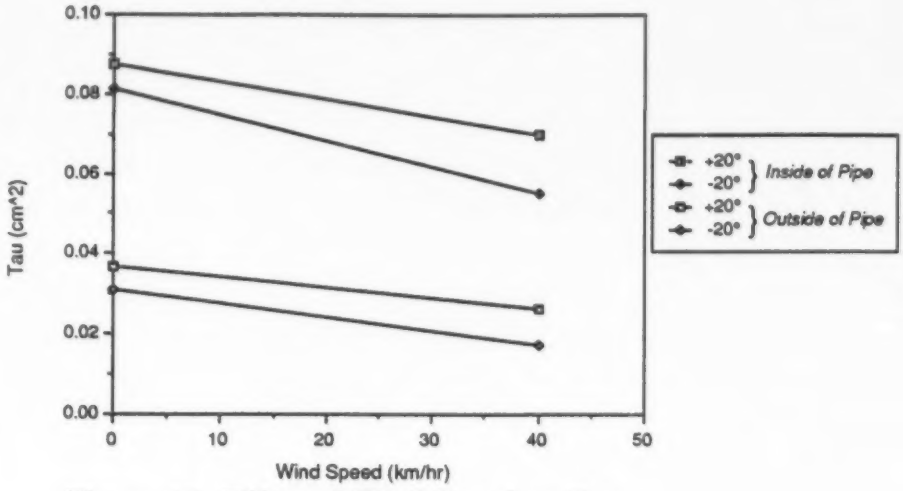

Figure 18 Effect of Wind Speed on Tau

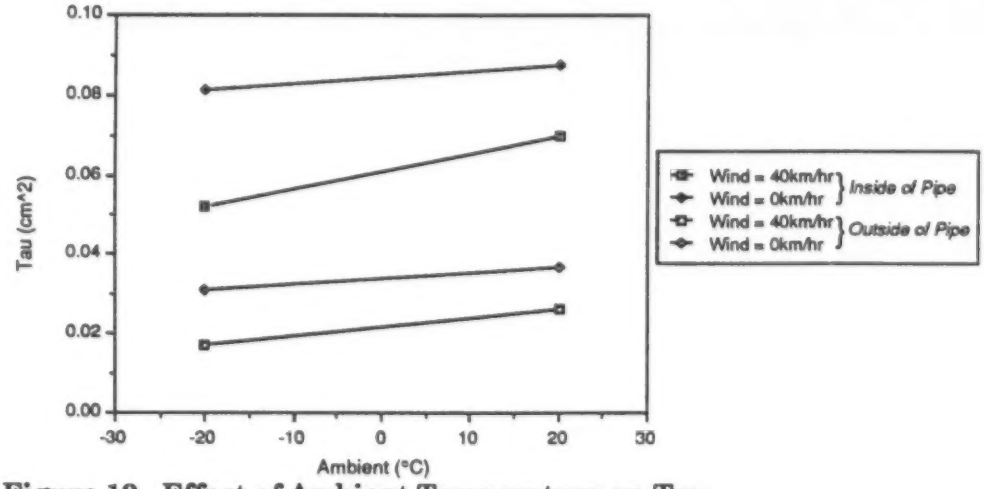

Figure 19 Effect of Ambient Temperature on Tau

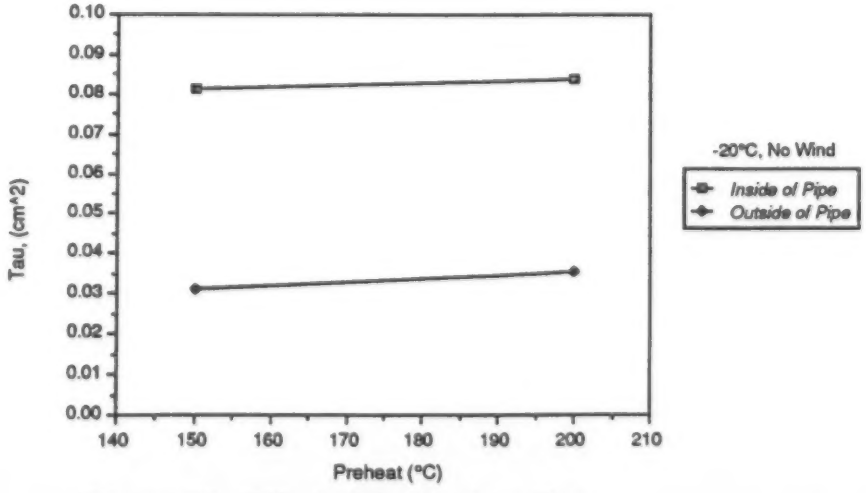

Figure 20 Effect of Preheat on Tau

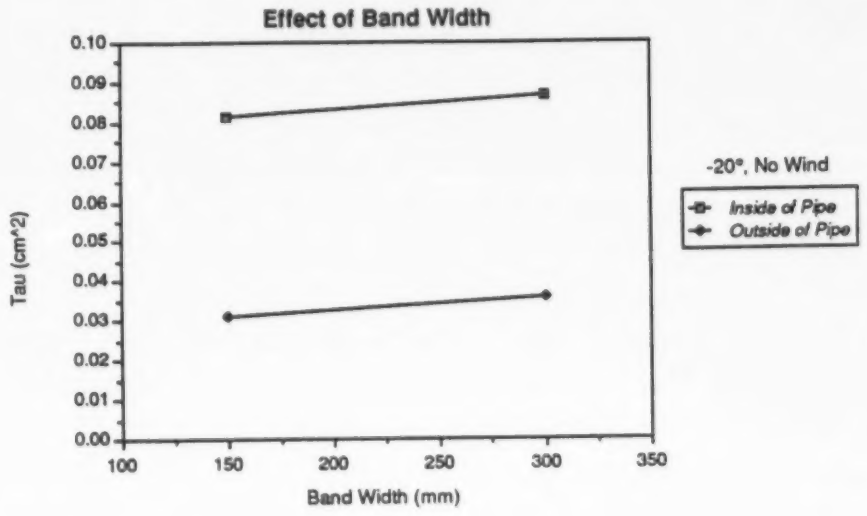

Figure 21 Effect of Band Width on Tau

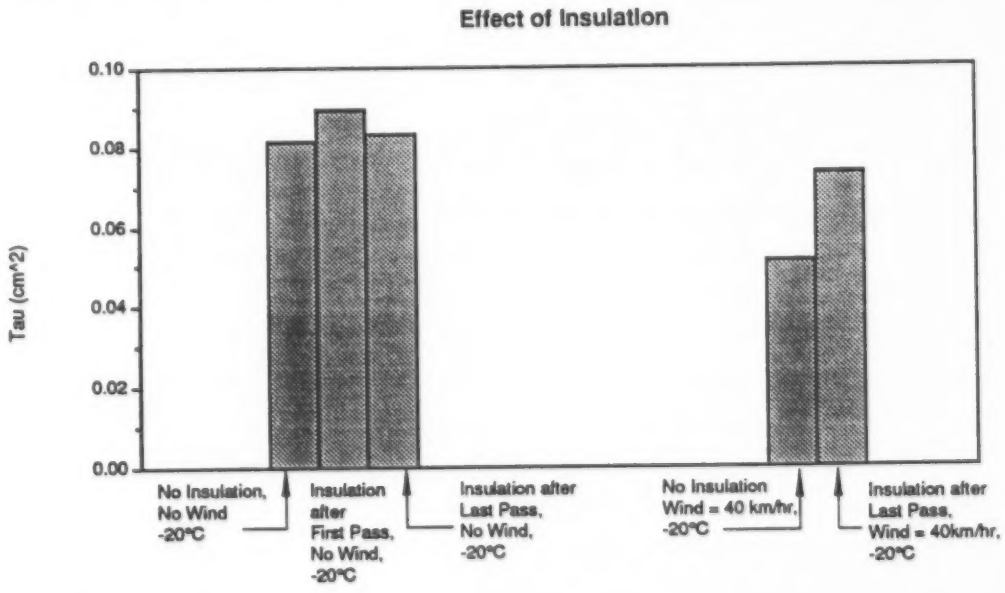

Figure 22 Effect of Insulation on Tau